TAMPERE UNIVERSITY OF TECHNOLOGY

Arto Hiltunen

Organic bulk heterojunction solar cells built on copper bottom electrodes

Master of Science Thesis

Examiner: Professor Donald Lupo
Examiner and subject approved
at the meeting of Faculty of Computing
and Electrical Engineering Council on
5 June 2013

TIIVISTELMÄ

TAMPEREEN TEKNILLINEN YLIOPISTO
Sähkötekniikan koulutusohjelma
Arto Hiltunen: Kuparielektrodien käyttäminen orgaanisissa P3HT:PCBM aurinkokennoissa
Diplomityö, 48 sivua
Syyskuu 2013
Pääaine: Vaihtoehtoiset sähköenergiateknologiat
Tarkastajat: Professori Donald Lupo ja tutkijatohtori Sampo Tuukkanen
Avainsanat: orgaaninen aurinkokenno, kupari, P3HT:PCBM, TiOx, ZnO, sinkkioksidi, cesium karbonaatti

Ilmastonmuutoksen hidastamiseksi EU velvoittaa jäsenmaitaan vähentämään hiilidioksidipäästöjään 30 % vuoteen 2020 mennessä sekä 60–80 % vuoteen 2050 mennessä vuoden 1990 tasoon verrattuna. Sähköntuotanto aurinkosähköpaneeleilla palvelisi päästövähennystavoitteiden saavuttamista. Tänä päivänä epäorgaanisilla aurinkokennoilla päästään helposti yli 30 % hyötysuhteisiin, mutta valmistukseen tarvittavien materiaalien korkea hinta ja valmistusprosessien hitaus ovat pitäneet paneelien hinnat korkealla. Kehittämällä orgaanista aurinkokennoteknologiaa, pyritään erityisesti nopeampiin valmistusprosesseihin ja tätä kautta aurinkosähköjärjestelmien huokeampaan hintaan. Nopean valmistuksen takaisi kennojen tuotanto tulostettavan elektroniikan menetelmin.

Tässä työssä tutkitaan kuparin soveltuvuutta orgaanisten aurinkokennojen elektrodimateriaaliksi. Tampereen teknillisen yliopiston Orgaanisen elektroniikan tutkimusryhmä on onnistuneesti valmistanut orgaanisia diodeja kuparielektrodien päälle tulostettavan elektroniikan menetelmin jo vuodesta 2009 lähtien. Sillä aurinkokenno on diodi, oli tämän työn tarkoituksena tutkia kuparielektrodin soveltuvuutta aurinkokennojen valmistukseen. Tutkimme aurinkokennojen valmistusta suoraan kuparielektrodin päälle ja lisäksi kokeilemme kuparin ja valoaktiivisen kerroksen välissä materiaaleja ZnO, Cs_2CO_3 ja TiO_x. Aurinkokennojen valoaktiivisena materiaalina käytetään P3HT:PCBM seosta.

ABSTRACT

TAMPERE UNIVERSITY OF TECHNOLOGY
Master's Degree Program in Electrical Engineering
Arto Hiltunen: Organic Bulk Heterojunction Solar Cells Built on Copper Bottom Electrodes
Master of Science Thesis, 48 pages
September 2013
Major: Alternative electrical energy technologies
Examiners: Professor Donald Lupo and Academy Postdoctoral researcher Sampo Tuukkanen
Keywords: organic solar cell, copper, P3HT:PCBM, titanium suboxide, cesium carbonate, zinc oxide

EU obliges its member states to reduce their greenhouse gas emissions by 30 % compared to that of 1990 levels by 2020 and further 60–80 % by 2050. Electricity production using solar panels would help to fulfill this obligation. Today inorganic solar cells can easily achieve energy conversion efficiencies as high as 30 % but the high price of inorganic solar panels has not made this technology popular. Motivation for developing organic solar cell technology is that it would allow the fast manufacture of panels and this way would lead to lower solar panel market prices. The fast manufacture is achieved using the developments of printed electronics.
This thesis studies the possibility to manufacture organic solar cells on copper electrodes. The Organic Electronics research Group of Tampere University of Technology has successfully manufactured printed organic diodes on copper since 2009. Because solar cell is a diode, we wanted to study the suitability of copper as a solar cell electrode material. We studied the manufacture of solar cells directly on copper but also ZnO, Cs_2CO_3 and TiO_x was tested in between the copper and the light active layer of the solar cell. The light active layer that we used was made of P3HT:PCBM blend.

PREFACE

I could not be happier that my experiments with the "raspberry solar cell" have led to the creation of this Master's Thesis about organic solar cells. I am extremely fortunate that it was Professor Donald Lupo who offered to help me with the raspberry project. Over the course of our collaboration, I have been graced with the opportunity to learn a great deal from him. His wisdom, expertise, support and guidance have aided me immeasurably in the process. The time I spent working in the Organic Electronics Group under his excellent supervision has granted me the most valuable insight into organic electronics. Many thanks also go to the whole OEG group for being such wonderful people and inspiringly talented engineers!

I would like to acknowledge the Supramolecular photochemistry research group of TUT led by Professors Helge Lemmetyinen and Nikolai Tkachenko for allowing me the best possible conditions for conducting the experimental component of my work in their laboratory. Special thanks go to the group's researchers who generously shared their wisdom in solar cell preparation with me.

My immense gratitude also goes to the whole personnel of the electromagnetics (SMG) group. Their ever helpful attitude, inspiring lectures and unwavering support has meant a great deal to me over the course of the past few years.

Thank you, Ossi Niemimäki, for so many things. There are far too many to list here, but they boil down into you being the most steadfast friend a person could hope to have. Let's have that pint and then let's down another, as that round's on me! Julia Johansson, it would be a crime against good manners and taste to leave your name out of this preface. You mean the world to me.

During the past years I've met a wide array of astonishing persons who live in different parts of the world and whose paths only occasionally intersect with mine. I can only hope that I took the chance to tell you that I loved you when I had it. This is a one such try.

I would like to thank my dearly loved family for offering me a stable home. Having an address that is not forever changing, one at which I am always welcome, is a profoundly beautiful thing.

As a final note I would like to thank the person who wrote this quote from Mark Twain on our kitchen wall. I think it was you, Ossi.

> Twenty years from now you will be more disappointed by the things you didn't do than by the ones you did do. So throw off the bowlines. Sail away from the safe harbor. Catch the trade winds in your sails. Explore. Dream. Discover.

Tampere, 16 August 2013 Arto Hiltunen

CONTENTS

SYMBOLS AND ABBREVIATIONS

Abbreviations

active	P3HT:PCBM active layer
C_{60}	buckminsterfullerene
DC	direct current
EIL	electron injection layer (hole blocking layer)
EQE	external quantum efficiency
evap	evaporated
FF	fill factor
HIL	hole injection layer (electron blocking layer)
HOMO	highest occupied molecular orbit
IQE	internal quantum efficiency
ITO	indium tin oxide
IV-curve	plot of current as a function of voltage
LiF/Al	aluminum electrode enhanced with lithium fluoride
LUMO	lowest unoccupied molecular orbit
MEA	monoethanolamine
MEH-PPV	Poly[2-methoxy-5-(2-ethylhexyloxy)-1,4-phenylenevinylene]
Milli-Q H_2O	ultrapure water
MIM	metal-insulator-metal
MPP	maximum power point
OC_1C_{10}-PPV	poly[2-methoxy-5-(3',7'-dimethyloctyloxy)-*p*-phenylene vinylene]
OLED	organic light emitting diode
PCB	printed circuit board
PCBM	[6,6]-phenyl-C61-butyric acid methyl ester

$PC_{70}BM$	[6,6]-phenyl-C71-butyric acid methyl ester
PCDTBT	poly[*N*-9”-hepta-decanyl-2,7-carbazole-alt-5,5-(4’,7’-di-2-thienyl-2’,1’,3’-benzothiadiazole)
PCPDTBT	poly[2,6-(4,4-bis(2-ethylhexyl)-4*H*-cyclopenta[2,1-b;3,4-b’]dithiophene)-*alt*-4,7-(2,1,3-benzothiadiazole)]
PEDOT:PSS	poly(3,4-ethylenedioxythiophene)-poly(styrenesulfonate)
PET	Polyethylene terephthalate
PLED	polymer light emitting diode
PPV	poly(*p*-phenylenevinylene)
PTAA	Poly[bis(4-phenyl)(2,4,6-trimethylphenyl)amine]
P3HT	poly(3-hexylthiophene)
rpm	rounds per minute
sol	solution process
TiO_x	titanium sub-oxide
TUT	Tampere University of Technology
UK	the United Kingdom
w%	weight percent

Symbols

c	speed of light
c	concentration
e	electron charge
eV	electron volt
$\overline{E}$	electric field
E_{ph}	photon’s energy
E_{g}	band gap
g	conductivity

h	Planck's constant
i	electric current
$i_{\max}$	current at MPP
I	electric current
I_{D}	current through a diode
I_{e}	current carried by the conduction band electrons
I_{h}	current carried by holes in the valence band
I_{L}	light generated current
I_{sc}	short circuit current
I_0	reverse saturation current
J	current density
k	Boltzmann constant
m	mass
n	number of electrons in the conduction band
n_{i}	intrinsic carrier concentration
p	number of holes in the conduction band
P	power
P_{in}	input power
$P_{\max}$	power at maximum power point
q	elementary charge
Q	number of quanta
R_{s}	series resistance
T	temperature
T_{s}	temperature of a black body radiator
u	voltage

$u_{\max}$	voltage at MPP
V	voltage
V_{oc}	open circuit voltage
x_{g}	variable
η	energy conversion efficiency
λ_{ph}	photon's wavelength
υ	photon's frequency
υ_{g}	minimum frequency required for photon absorption
φ	work function
ΔV	voltage loss
ΔV_b	sum of the voltage losses due to the band bending
$\Omega/\square$	sheet resistance

1. INTRODUCTION

Climate Change 2007 Synthesis Report[1] provided by the IPCC (Intergovernmental Panel on Climate Change) says that warming of the climate system is certain and it is driven by increased concentrations of greenhouse gases in the atmosphere which are due to human activity. IPCC estimates that increase of the average global temperature in the year 2090-2099 compared to that in 1980-1999 will be between 1.1 to 6.4 degrees Celsius depending on the development scenario [1, p. 45].

The impacts of global warming will be mostly negative. Tendencies for some cereal production is previsioned to increase at mid- to high latitudes when the increase in temperature is less than 3 °C. However "At lower latitudes, especially in seasonally dry and tropical regions, crop productivity is projected to decrease for even small local temperature increases (1 to 2 °C)". Also it is stated that "The negative impacts of climate change on freshwater systems outweigh its benefits". [1, p. 48–49]

European Union has decided to take measures against the climate change. A serious negative impact on the society could be avoided, according to the European Union, by limiting the increase in temperature below 2 °C. The concrete measures to meet the objective would be to reduce the greenhouse emissions of the EU Member States by 30 % compared to that of 1990 levels by 2020 and furthermore to reduce the emissions by 60 to 80 % by 2050. [2]

All this said above shall serve us as a motivation for developing photovoltaic technology since solar cells can provide us a greenhouse gas emission free way for producing electricity. We would like to emphasize here that we see the solar energy production only as a *one* contribute to the whole energy production along with other energy sources.

Classical silicon-based solar panels have proven to be efficient and stable technology even to such extent that crystalline silicon in conjunction with other inorganic photovoltaic materials, namely gallium arsenide, have become the standard choice for power in deep-space applications [3]. However the high manufacture costs limit the popularity of these technologies on Earth. Organic solar cell technology is aiming to allow low cost production of solar panels.

Solar cells considered in this work fall under the class of *organic photovoltaics*

[1]Next, the fifth report, is expected to be published in 2014.

and the word organic suggest that the active material in the cell contains carbon atoms. The basis for this technology is the discovery of photoconductive polymers in the late 1970s which gave the Nobel price in Chemistry in 2000 to the researchers.

The major strength of the organic photovoltaic technology is the possibility of preparing parts of the cell — if not the whole cell — using printing technologies. Printing would allow fast and high yield production which would mean low manufacturing costs if the materials themselves were not too expensive. This is also the reasoning behind this work as we were seeking a way to use copper as a electrode material instead of ITO which is today a common choice in organic solar cell technology.

Printing on flexible substrates would allow the solar cells, too, be flexible which again broadens the set of applications where the technology could be implemented. Also organic solar cells can be made semi-transparent and different colors. These three last mentioned properties are a major advantage when considering applications in buildings or other environments where the aesthetic aspects also matters.

In chapter 2 the basic theory required to understand the working principles of the solar cells considered in this work is given. In chapter 3 we present the electrode materials, interlayer materials and the active layer materials. Also, a detailed presentation of the preparation of the layers is given. In the end of the chapter the measurement set up is described. In chapter 4 we give the results and discuss possible causes for the observations. Conclusions are given in chapter 5.

2. THEORETICAL BACKGROUND OF SOLAR CELLS

In this chapter the theory of solar cell technology is presented to such extent that a reader should understand the working principles of solar cells in general and then the functioning of polymer/fullerene solar cells as a special case. Along with theory we give some history, introduction to organic electronics and engineering aspects of polymer/fullerene solar cells.

2.1 Power generation

A photovoltaic cell — solar cell — is a device that can convert light into electricity. We could also say that it is *a device that can under illumination provide electric power to a load.* The power P is defined by equation

$$P = VI,$$

where V is the voltage provided by the solar cell over the load and I is the electric current through the load.

To be able to provide power, a solar cell must consist of something that reacts to light such way that charge carriers are generated which can be collected at electrodes and then fed into a circuit. That one sentence description just given might seem vague but it contains just the two essential aspects that make a solar cell: i) *creation of free charge under illumination* and ii) *collection of charge.* Many devices or materials do one or the other but not both.

We use the term free charge in the sense that a charge is free to contribute to the current flow. Doing this we avoid saying that we would actually create charges and are thus consistent with the statement that the net charge is preserved in a closed system [4, p. 27]. For now we shall be talking about charge or charges without explicitly specifying what we mean by them. We shall define more precisely our vocabulary in section 2.1.1.

A schematic diagram of a solar cell is presented in figure 2.1. Creation of free charges takes place in the active layer and collection of charges is done by electrodes.

The amount of current that a solar cell can feed into a circuit depends on the amount of light incident on the cell. In an ideal case every photon incident on the

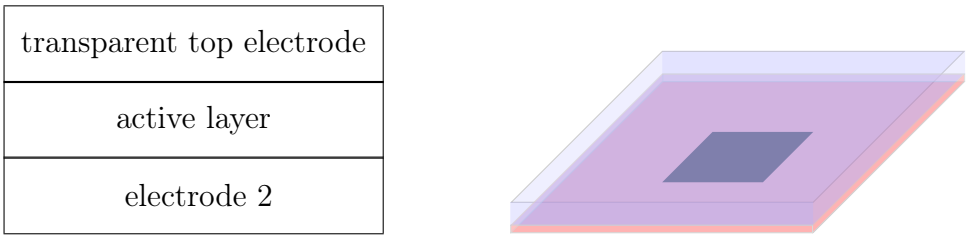

(a) (b)

Figure 2.1: The figure on left tries to give an idea of the minimum requirements of what one might need to build a solar cell. On right is a sketch of a solar cell that one might prepare in a laboratory. The structure is (from top to bottom) glass|transparent electrode|active layer|electrode 2. In this particular case the active *area* is determined by the area of the electrode 2 (the gray square in the middle).

active layer would contribute to the charge generation. However since a photon's energy depends on its wavelength, not every photon possesses enough energy to create free charges. How much energy is needed for the creation of free charges in a material is a material property. Also the active layer materials today are limited by their absorbance in a way that they only absorb a part of the solar spectrum. This means that even if a high energy photon was incident on the cell it might not be absorbed. Internal quantum efficiency (IQE) and external quantum efficiency (EQE) are quantities that measure the charge production capability of a cell under illumination. They are defined as a function of wavelength the following way [5]

$$IQE = \frac{\text{charge collected at electrodes}}{\text{photons absorbed by the active layer}}$$

and

$$EQE = \frac{\text{charge collected at electrodes}}{\text{photons incident on the active layer}}.$$

While IQE and EQE look at the behavior of the cell one wavelength at a time, as a whole the solar cell is characterized by its *efficiency*, η, defined as

$$\eta = \frac{P_{\text{max}}}{P_{\text{in}}},$$

where P_{in} is the solar power incident on the active area of the cell and P_{max} is the maximum power output.

Every solar cell has a characteristic IV-curve (see fig.2.2) that tells us how much power can be attained from the cell at given point of operation (u, i) on the IV-curve.

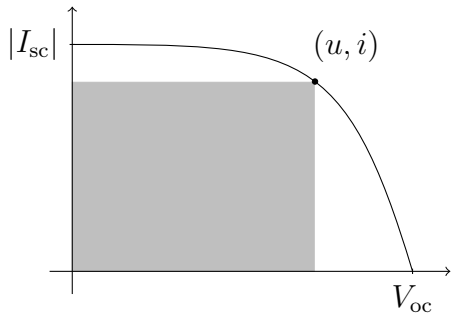

Figure 2.2: A typical shape of an IV-curve. Geometrically the maximum power point is the point on the IV-curve that maximizes the gray square drawn in the figure.

The point which provides the maximum power, P_{max}, is called the maximum power point which we denote as (u_{max}, i_{max}). From the IV-curve we can calculate the fill factor FF from equation [6, p. 80]

$$FF = \frac{u_{max} i_{max}}{V_{oc} I_{sc}},$$

where V_{oc} is the open circuit voltage and I_{sc} the short circuit current. Ideally the solar cell IV-curve would be a square determined by V_{oc} and I_{sc}, meaning that the solar cell could produce a high output current also at high voltages near V_{oc}. Typically the current values are low near V_{oc} as depicted in figure 2.2. Thus the fill factor measures how close the solar cell is to an ideal device.

2.1.1 Some basic concepts of semiconductor theory

Semiconductor characteristics

Electrical properties of semiconductors lie somewhere between those of insulators and conductors: in normal conditions semiconductors usually conduct poorly but when energy is added into the system the conductivity can be increased by several orders of magnitude. This behavior is explained by introducing the concepts of energy bands and band gap.

Electrons in an isolated atom are restricted to a set of discrete energy levels. In a semiconductor crystal atoms are in close contact and as a consequence the energy levels of individual atoms interact forming *energy bands* where the discrete energy levels of individual atoms are so densely packed that the band appears to have a continuous distribution of energy levels. [6, p. 17] The same way as the electron of an isolated atom cannot have an energy value outside the set of allowed energies, electrons in a semiconductor crystal cannot be found outside the bands. The highest energy band occupied by electrons is called the *valence band* and the next empty band is called the *conduction band*. The difference between the highest energy level

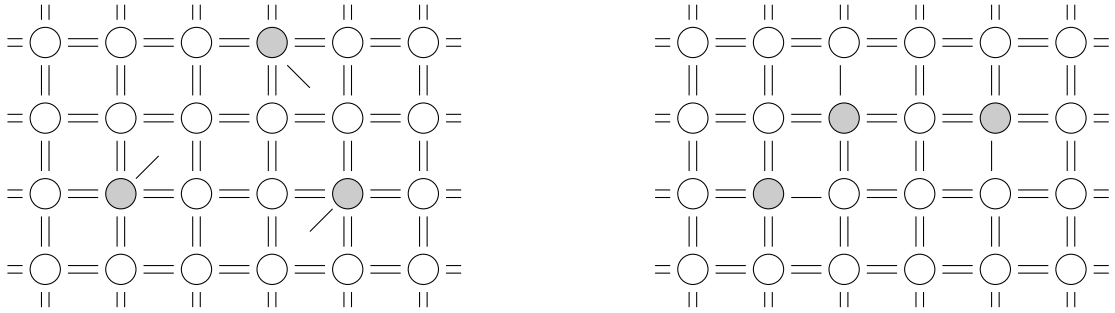

(a) n-type (b) p-type

Figure 2.3: The effect of dopants in a semiconductor crystal. The dopant atoms are colored gray.

of the valence band and the lowest level of the conduction band defines the *band gap*.

What differentiates a semiconductor from an insulator is the size of the band gap. The band gap of an insulator is so great that electrons cannot be excited to the conduction by adding energy to the system. But when sufficient energy is added to a semiconductor crystal the electrons in the valence band are able to jump the gap, enter the conduction band and contribute to the current flow. [7, p. 1598]

Electric current is flow of charges. By saying that the conduction band is empty and the valence band is full, we mean that all the electrons are used to make bonds with the neighboring atoms and are thus bound to the crystal; they can't move around; they are not *free* to carry current. Breaking a bond frees an electron, so we say that is has entered the conduction band. [8, p. 158–159], [6, p. 18–20]

Semiconductor properties by can be altered by adding substituents also know as dopants into the semiconductor crystal. Dopants are atoms that contain more or less valence electrons than the atoms that make up the semiconductor crystal. For example phosphorous and boron which contain five and three valence electrons respectively can be used to dope silicon which has four valence electrons.

In a silicon crystal, silicon uses its four valence electrons to make covalent bonds with the neighboring Si-atoms. Also phosphorous in the Si-crystal uses four of its valence electrons to make the covalent bonds, leaving the fifth electron free. To be precise, this fifth electron is hold back by the positive charge in the phosphorous nucleus, but this interaction is very weak and the electron can be freed with a very small amount of energy (≈ 0.02 eV) [6, p. 29]. Because the free electrons coming from phosphorous can easily contribute to the current flow, they are usually drawn directly to the conduction band of the crystal in a band diagram. The act of adding negative charge carriers into a semiconductor is called n-type doping. Atoms that donate the electrons are called donors.

Addition of boron in a Si-crystal leaves "a hole" into the crystal because boron

has only three valence electrons that can be used to make bonds with silicon. An electron that is covalently bound in the crystal can move into a hole, which moves the hole in that place where the electron originally was [9]. Thus the movement of an electron can be seen as the movement of a hole and vice versa, from which follows that we can consider the movement of holes as a contribute to the current flow.[1] In the energy band diagram, holes are drawn into the valence band or in the direct vicinity [6, p. 29]. Engineering holes into a semiconductor is called p-type doping, and the p-type dopants are called acceptors since they accept the electrons from the adjacent atoms. [8, p. 159–160] The effect of dopants is illustrated in figure 2.3. Because this phenomenon is of personal interest, the discussion is ended with a direct quote from Pearson and Bardeen: [9, p. 866]

> The missing electron, or hole, behaves in all respects like a particle with a positive charge equal in magnitude to the electron charge. It has inertia, momentum, and energy corresponding to a mass of the same order as the mass of an electron. – – The only essential difference is in the sign of the mobile charge.

Majority and minority charge carriers

The way doping effects the energy band diagrams is presented in figure 2.4. N-type doping increases the number of conduction band electrons and p-type doping introduces holes into the valence band. Figure 2.4(a) shows the situation in an intrinsic (i.e. undoped) semiconductor relative to the doped ones. For an idealized intrinsic semiconductor holds [6, p. 26]

$$n = p = n_{\mathrm{i}},$$

where p is the number of holes in the valence band, n is the number of electrons in the conduction band and n_{i} is called the intrinsic carrier concentration that has been measured to be $1.00 \cdot 10^{10}$ cm^{-3} for silicon [11].

The definitions for majority and minority charge carriers are established from figure 2.4. In the n-type semiconductor the major part of the current is carried by the conduction band electrons, while the holes in the valence band have a smaller contribution to the current. Thus, we define that in a n-type semiconductor electrons in the conduction band are majority carriers and holes in the valence band are minority carries. Using the same logic, we define that in a p-type semiconductor the holes in the valence band are majority carriers and electrons are minority carriers.

[1] Note however that the *only charge carriers are electrons* but sometimes, if we decide to do so, we may regard the flow of electrons as the flow of fictious particles called holes [10, p. 226]. We will often choose to do so. For a more profound treatment the reader is referred to [10].

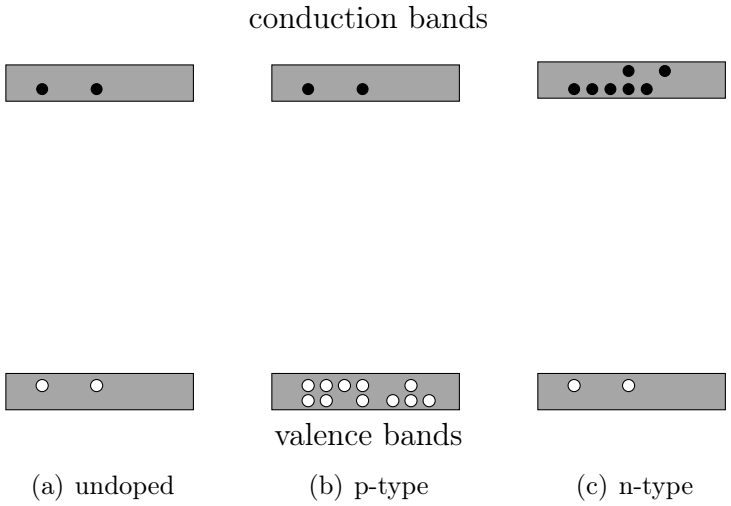

(a) undoped (b) p-type (c) n-type

Figure 2.4: The effect of doping semiconductors. P-type semiconductor has an increased number of holes in the valence band and the n-type semiconductor has an increased number of free electrons in the conduction band. In reality the number of holes and electrons in an undoped semiconductor is around $1 \cdot 10^{10}$ cm^{-3}.

[12, p. 84–85]

The total current density J in a semiconductor is given as

$$J = J_\mathrm{e} + J_\mathrm{h},$$

where J_e is the current carried by conduction band electrons and J_h is the current carried by holes in the valence band [6, p. 34]. Notice that charges of opposite signs must flow in opposite directions in order to contribute to a current flow in the same direction. This is a corollary of the definition of electric current [4, p. 163].

The pn-junction

The pn-junction is the basis for several electronic devices, also for solar cells. As the name suggest, a pn-junction is formed by joining a p-type and a n-type semiconductor together. When the junction is formed, the free electrons near the junction in the n-type side diffuse into the holes near the junction in the p-type side. The n-type dopant atoms near the junction that lost electrons in the diffusion process become positively charged. Similarly, the p-type dopants that accepted the diffused electrons become negatively charged. This charging forms a potential across the junction that eventually prevents a further flow of charge. We can model the potential with an electric field that is directed from n-side to p-side. [12, p. 170]

By definition the direction of an electric field is such that it points at the direction where the flow of positive charge is assisted. It follows that in a pn-junction the formed electric field opposes the flow of holes from the p-side to the n-side and the

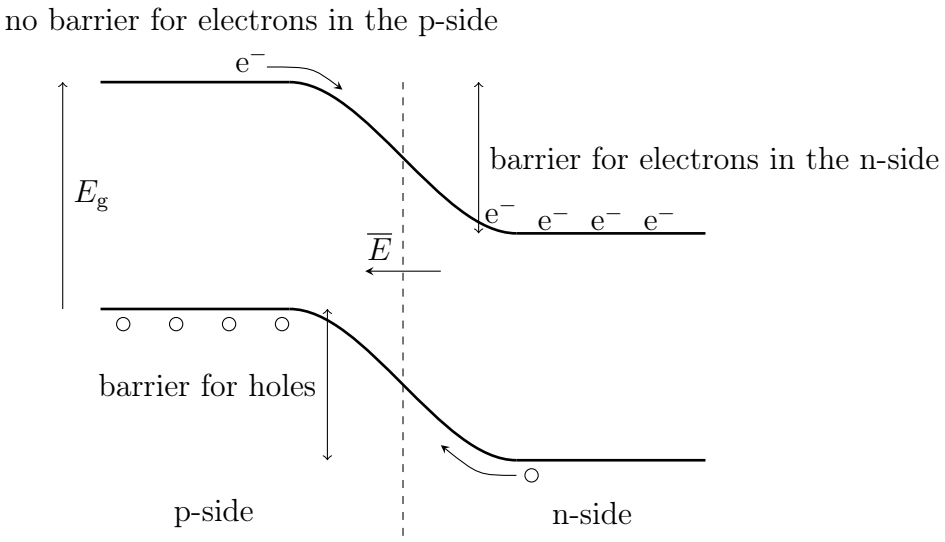

Figure 2.5: The energy bands of a pn-junction. The dashed line in the middle shows the junction and E_g is the band gap of the semiconductor. Superimposed is the direction of the electric field $\overline{E}$ inside the junction.

flow of electrons from the n-side to the p-side. Hence, the electric field opposes the flow of majority charge carriers across the junction. But both sides contain a small density of minority charge carriers, electrons in the p-side and holes in the n-side, that are aided across the junction by the electric field.

Another way to explain the functioning of a pn-junction is to consider the energy bands across the junction. In figure 2.4 we drew the energy bands with a *straight* gray block. When a pn-junction is formed, the energy bands *bend*. The situation is illustrated in figure 2.5. We see that due to the band bending the majority charge carriers on both sides feel a barrier that they should cross in order to get to the other side of the junction. The minority charge carriers feel no barrier on either side. [7, p. 1610], [12, p. 170–171]

The flow of charge carriers across the junction can be controlled by applying a *bias voltage* across the junction. Forward biasing a pn-junction means applying a positive voltage on the p-type side of the junction and negative on the n-type side. Forward biasing assists the flow of majority charge carriers over the junction while reverse biasing decreases the flow of majority charge carriers. [8, p. 160–163]

2.1.2 The shape of an IV-curve

In this section we shall try to find an explanation for the shape of an IV-curve of a solar cell. It is possible to measure two different IV-curves: one under illumination and one in dark.

The dark curve of a solar cell resembles the IV-curve of *a diode* and obeys thus well the diode equation [12, p. 184]

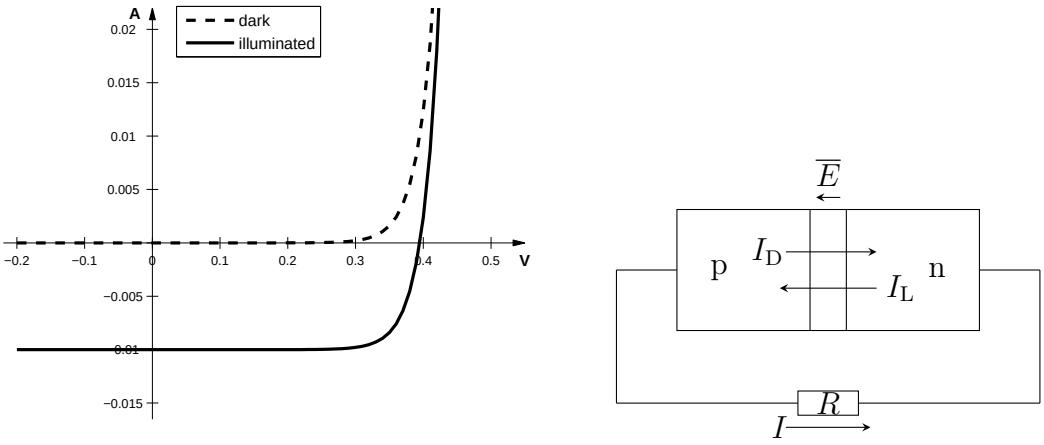

(a) (b)

Figure 2.6: a) Plots of equations 2.1 (dashed) and 2.3 (solid line) as a function of V. $I_0 = 10^{-9}$ A, $I_L = 10$ mA, $T = 300$ K, $V \in [-0.2, 0.6]$. b) Currents in an illuminated pn-junction and the net current I.

$$I_D = I_0(e^{qV/kT} - 1) \tag{2.1}$$

where, I_D is the current through the diode, V is the voltage over the diode, I_0 the reverse saturation current, q the elementary charge, k the Boltzmann constant ($\approx 1.381 \cdot 10^{-23}$ J/K) and T the temperature. Indeed, solar cells are diodes apart from the differences in the optical properties. The graph of I_D is plotted in figure 2.6(a) with dashed lines. It's important to notice that I_D consists mostly of *majority charge carriers*.

Photons that have energy greater than the band gap of the semiconductor material will increase the number of minority and majority charge carriers on both, p and n, sides but only the minority charge carriers are aided across the junction by the $\overline{E}$-field. As a result a light generated current, I_L, that consists of the increased number of minority charge carriers that drift across the junction, grows greater than I_D and the IV-curve falls into the fourth quadrant in figure 2.6(a). While the bias voltage is increased in the forward direction, more and more majority charge carriers are flowing across the junction and I_D is suddenly increased over I_L. Directions of I and I_D are shown in figure 2.6(b).

When the solar cell is operated in the fourth quadrant the product of current and voltage becomes negative, which means that power is extracted from the solar cell. Based on the discussion above we can present the first model for the IV-curve of a solar cell as

$$I = I_{\mathrm{D}} - I_{\mathrm{L}} \tag{2.2}$$
$$= I_0(\mathrm{e}^{\mathrm{q}V/\mathrm{k}T} - 1) - I_{\mathrm{L}}. \tag{2.3}$$

I_{D} and I are plotted in figure 2.6(a). Equation 2.3 was proposed as early as 1955 by Bell Telephone Laboratories that had build the very first silicon based pn-junction solar energy converter one year earlier [13].

To be precise, in the original publication [14] equation 2.3 was to describe an equivalent circuit model for a solar cell that would consist of a diode (I_{D}) connected in paraller with a constant current source (I_{L}). Most of the time this circuit is still the basis of equivalent circuit models that try to describe the behavior of any modern solar cell: dye-sensitized [15] or organic [16].

2.2 Charge generation in the active layer

This thesis is dealing with devices whose active layer is made of donor and acceptor materials, namely from polymer and fullerene respectively. Next we describe the functioning of this type of active layer in more detail. (See section 2.4.2 to find out how we and others have come to this choice of active layers). We draw some analogy between organic and inorganic semiconductor theory.

Solar cells are energy converters[2] and they are able to do this conversion due their ability to *absorb* photons of certain energy and transfer that energy to electrons in a semiconductor. A photon's energy, E_{ph}, is given as [7, p. 1453]

$$E_{\mathrm{ph}} = \frac{\mathrm{hc}}{\lambda_{\mathrm{ph}}} = \mathrm{h}\upsilon,$$

where h is the Planck's constant, c the speed of light, λ_{ph} the photon's wavelength and υ the photon's frequency.

Probability for a photon absorption is high if the photon's energy is higher than the band gap of the semiconductor. Absorption of photons with smaller energies is low because inside the band gap there is no allowed states where the electron could be excited. When a photon is absorbed by the semiconductor it increases the electron's energy by the amount of its own energy, E_{ph}, so that the electron can leave the valence band and enter the conduction band. The electron that has quit the valence band leaves behind a hole. Thus absorption of a photon leads to creation of an electron-hole pair. [12, p. 119] The photon absorption process is illustrated in figure 2.7(a).

[2] In fact the first modern articles in 1950s that were written about the topic talked about "solar energy converters" rather than solar cells. See for example [14].

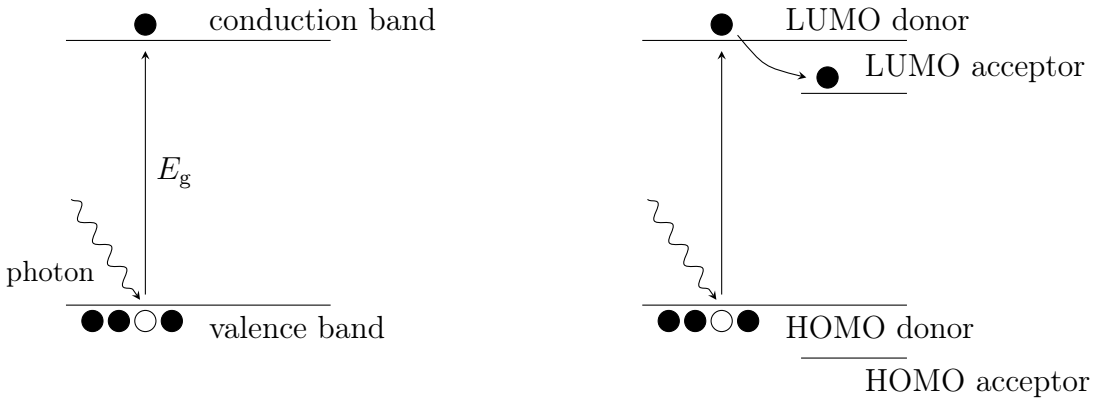

(a) Inorganic semiconductor

(b) Organic donor-acceptor heterojunction

Figure 2.7: Band diagrams and photon absorption in inorganic and organic semiconductors.

Using the language of organic chemistry it is common practice to talk about HOMO (highest occupied molecular orbit) and LUMO (lowest unoccupied molecular orbit) levels instead of valence and conduction bands. However the schematic presentation of electron transfer between the levels or bands is very similar as can be seen comparing figures 2.7(a) and 2.7(b). It can be seen that when the active layer is constructed from two materials, donor and acceptor, the electron is transferred from donor to acceptor.

2.2.1 The bulk heterojunction active layer

Absorption of a photon in an inorganic semiconductor leads directly in creation of an electron-hole pair [17]. However in organic semiconductors the formation of an electron-hole pair is proposed to happen via successive steps which we must consider if we are aiming to build efficient solar cells. Despite the debate[3] within the scientific community concerning the steps of this process we next present one sequence that describes the charge generation in polymer/fullerene solar cells that is provided in reference [19]. We will look into more detail at a special kind of active layer called the bulk heterojunction.

According to [19], absorption of a photon by the polymer (donor) creates an exciton which can move about in the donor phase a distance called the exciton diffusion length. If the exciton encounters a donor-acceptor interface before decaying it is transformed into a electron-hole pair, that might still be Coulombically bound, where the electron is in the acceptor phase and the hole in the donor phase. The electron-hole pairs are then separated into free charges with the aid of electrodes;

[3]Pointed out for example by Dennler and Sariciftci in [18].

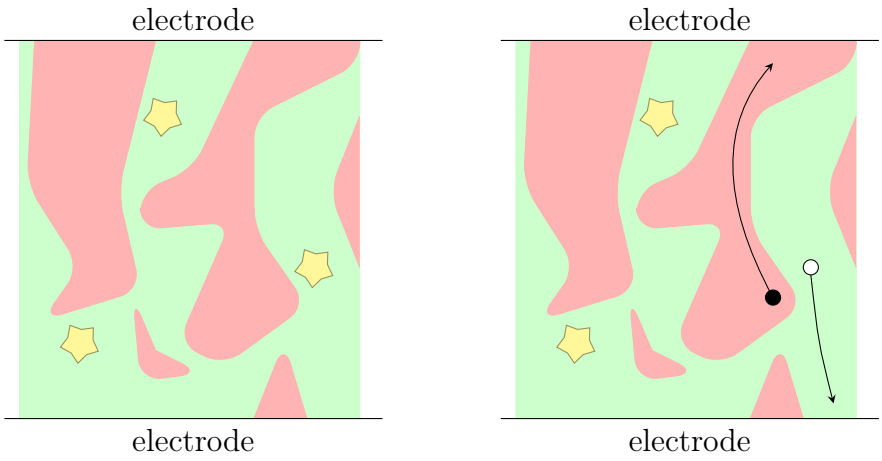

Figure 2.8: Author's illustration of the bulk heterojunction. Stars present the excitons created in the donor(polymer) material by photons. Donor material is colored green and acceptor material red. On right, one of the excitons has reached a donor-acceptor interface and separated into a electron-hole pair. Electron is drawn with the black circle and hole with white circle.

anode collecting the hole and cathode collecting the electron.

A source for controversy has been whether the excitons dissociate into Coulombically bound electron-hole pairs or directly into free charge carriers. In reference [20] it is concluded that in P3HT/PCBM devices the exciton dissociation leads directly into a formation of free charge carriers but in reference [21] the authors, three of whom also contributed to the previous article, conclude that in PCPDTBT/$PC_{70}BM$ devices the electron-hole pairs are Coulombically bound. Thus, it seems that the question is actually case dependent.

The bulk heterojunction is described to consist of a network of internal donor-acceptor heterojunctions. Because separation of excitons into electron-hole pairs happens at the donor-acceptor interface, the idea behind bulk heterojunctions is that there would always be an interface within the exciton diffusion length [22] which is estimated to be around 14 nm [23]. The charge separation process in bulk heterojunction solar cells is illustrated in figure 2.8.

Although the structure might seem complex, the functioning of the bulk heterojunction active layer can be analyzed using the energy level concept depicted in figure 2.7. Moreover, for modeling purposes the bulk heterojunction has been thought to be just one semiconductor; the HOMO level of donor being equivalent to the valence band and LUMO level of acceptor being the conduction band. This approach has been used for example in reference [24].

2.2.2 Ultimate efficiency

We shall next consider the ultimate efficiency of a solar cell. More precisely, we shall present an approximation for the amount of energy that could be harvested from solar irradiation using one pn-junction — using one band gap. The analysis will be based solely on the celebrated article by Shockley and Queisser from 1961 [25]. Although their analysis concerns inorganic devices, that were under intense study at the time, we see no reason why this analysis wouldn't apply to organic devices within the frame of the assumptions that have been made. The assumptions are

1. The solar cell has a circular shape and it is surrounded by a blackbody of temperature T_s. See figure 2.9.
2. The solar cell is held at temperature 0 K.
3. Only photons that have energy greater than the semiconductor band gap are absorbed. The amount of energy that is absorbed equals the band gap of the semiconductor.

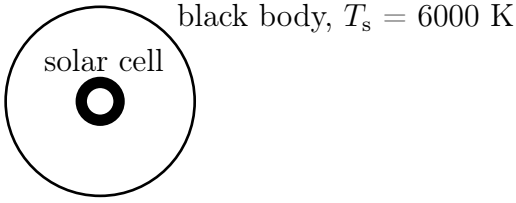

Figure 2.9: Solar cell and radiation source geometries.

Photons with different energies arrive in different amounts. The idea of the ultimate efficiency calculation is to find that band gap value which can absorb those photons that carry the largest portion of the available energy. A small band gap semiconductor will absorb a large part of the irradiation spectrum but the amount of energy that is harvested for energy production stays low because the amount of the photon's energy that exceeds the band gap is lost in the semiconductor lattice in scattering events. [12, p. 119] The idea is elucidated in figure 2.10.

The calculation begins with considering the number of quanta Q ($\mathrm{m^{-2}s^{-1}}$) that have a energy greater than the band gap $E_\mathrm{g} = \mathrm{h}\upsilon_\mathrm{g}$. This equals the number of absorbed photons. Q is calculated by integrating the Planck distribution from υ_g to infinity:

$$Q = \frac{2\pi}{\mathrm{c}^2} \int_{\upsilon_\mathrm{g}}^{\infty} \frac{\upsilon^2}{\mathrm{e}^{\mathrm{h}\upsilon/\mathrm{k}T} - 1} \, \mathrm{d}\upsilon. \tag{2.4}$$

It is possible to simplify the integrand by introducing a new symbol, x_g, defined as $x_\mathrm{g} = \frac{\mathrm{h}\upsilon_\mathrm{g}}{\mathrm{k}T}$. Substituting x_g along with $\mathrm{d}x = \frac{\mathrm{h}}{\mathrm{k}T}\mathrm{d}\upsilon$ into 2.4 gives

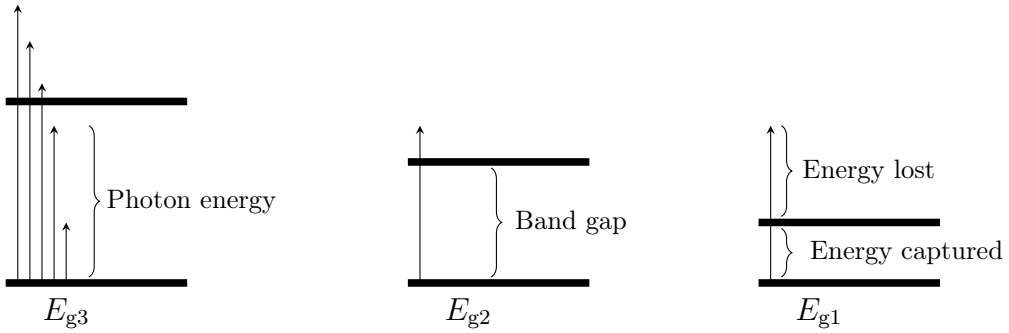

Figure 2.10: The height of the arrow describes the energy of the incident photon. For the band gap values apply $E_{g3} > E_{g2} > E_{g1}$.

$$Q = \frac{2\pi(\mathrm{k}T)^3}{\mathrm{h}^3\mathrm{c}^2} \int_{x_\mathrm{g}}^{\infty} \frac{x^2}{\mathrm{e}^x - 1}\,\mathrm{d}x.$$

The total energy carried by the quanta, originating from the black body, can be calculated from 2.4 by multiplying the formula with $\mathrm{h}\upsilon$ and integrating it over the whole frequency range from zero to infinity:

$$P_\mathrm{in} = \frac{2\pi\mathrm{h}}{\mathrm{c}^2} \int_0^{\infty} \frac{\upsilon^3}{\mathrm{e}^{\mathrm{h}\upsilon/\mathrm{k}T} - 1}\,\mathrm{d}\upsilon,$$

which yields the Stefan-Boltzmann law [7, p. 1475]

$$= \frac{2\pi^5(\mathrm{k}T)^4}{15\mathrm{h}^3\mathrm{c}^2}.$$

Now we are ready to calculate the efficiency η as a function of x_g from equation

$$\eta(x_\mathrm{g}) = \frac{P_\mathrm{out}}{P_\mathrm{in}} = \frac{h\upsilon_\mathrm{g} Q(x_\mathrm{g})}{P_\mathrm{in}},$$

where P_out is the output power of the solar cell that is estimated to equal the amount of photons absorbed times the energy that can be harvested per photon.

In [25] a neat analytical solution is found for 2.4. We chose to perform the calculations numerically using MATLAB. The results are given in figure 2.11. The ultimate efficiency 44 % is found at x_g= 2.2 which corresponds to a band gap value of about 1.1 eV, which could be calculated from relation

$$x_\mathrm{g} = \frac{\mathrm{h}\upsilon_\mathrm{g}}{\mathrm{k}T_\mathrm{s}} = \frac{\mathrm{q}V_\mathrm{g}}{\mathrm{k}T_\mathrm{s}}.$$

The band gap of silicon is approximately 1.1 eV [41, p. **12**–80] which makes silicon an optimal material for solar energy conversion in the light of this analysis. In

organic bulk heterojunction solar cells the difference between the donor HOMO level and acceptor LUMO level is approximately 1.9 eV which gives 33 % for ultimate efficiency. Based on the assumptions of this section, a significant improvement in the organic solar cell conversion efficiency could be expected if the LUMO and HOMO levels of the active layer materials could be engineered to give a smaller "band gap". However our analysis is very much simplified. The optimum band gap value will be different from 1.1 eV when more variables are taken into account. A more detailed analysis is also included in [25].

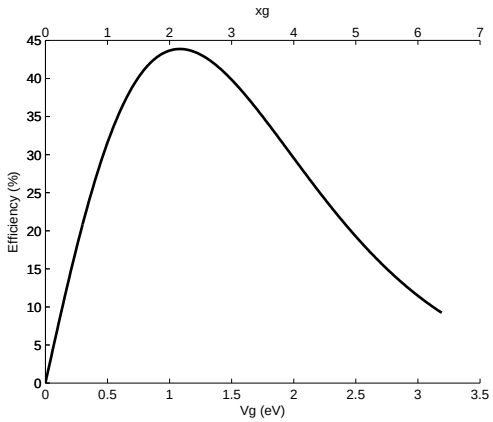

Figure 2.11: Ultimate efficiency

2.3 Electrodes and voltage

So far we have concentrated on the free charge creation in the active layer and have not said much about the collection of charge, except that it happens at electrodes. We look at that part now.

In the solar cells under study the current is carried by both electrons and holes. In order to make the charges of opposite signs contribute to the net current flow in the same direction, the charges — electrons and holes — must be lead to opposite directions in the device. This is a corollary of the definition of electric current [4, p. 163]. The situation is established by choosing electrodes with different *work functions* [19]. Holes diffuse towards the electrode with higher work function and electrons towards the electrode with lower work function (see figure 2.12).

The way electrode work functions are situated relative to the HOMO and LUMO levels of the semiconductor results in two different contact types between the materials : ohmic and non-ohmic.

When the work function, φ, of an electrode is below the LUMO level of acceptor or above the HOMO level of donor (such as depicted in fig. 2.12(a)) are the metal-semiconductor contacts said to be non-ohmic. In this case the maximum attainable voltage, V_{oc}, is obtained from the work function difference of the electrode materials

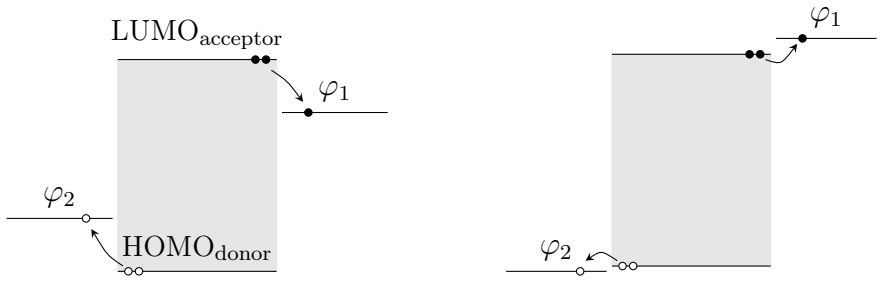

(a) non-ohmic contacts (b) ohmic contacts

Figure 2.12: Two different metal-semiconductor contacts are shown. In addition the flow of free charge carriers in the device is pictured.

which is in accordance with the metal-insulator-metal (MIM) model for solar cells. [26] Written into an equation we get

$$V_{\text{oc}} = \frac{\varphi_2 - \varphi_1}{\text{q}}, \tag{2.5}$$

where φ_2 and φ_1 are the electrode work functions and q is the elementary charge.

If the electrode work functions are *close* to the donor HOMO and acceptor LUMO levels as in fig. 2.12(b) an ohmic contact is formed. Each ohmic contact contributes a voltage loss, ΔV, which reduces the maximum obtainable voltage from the solar cell. The voltage loss is explained to be caused by accumulated charges at the contact which results in energy level band bending in the semiconductor. [26] We write this into an equation[4] the following way

$$V_{\text{oc}} = \frac{\text{HOMO}_{\text{donor}} - \text{LUMO}_{\text{acceptor}}}{\text{q}} - \Delta V_b, \tag{2.6}$$

where ΔV_b is the sum of the voltage losses due to band bending and the HOMO and LUMO levels are supposed to be given as absolute values. In ref [27] Scharber et al. test 26 different bulk heterojunction solar cells and end up experimentally in an equation for V_{oc} which is similar to equation 2.6.

2.4 Organic electronics

Organic electronics is a field that extends over a broad set of applications which include organic photovoltaics, flexible displays, lighting products, electronics & components and Integrated Smart Systems as illustrated in figure 2.13. To define what is meant by organic electronics we quote the OE-A Roadmap [28, p.4]

> Organic electronics is based on the combination of a new class of mate-

[4] In ref [26] the authors give this equation to a particular device, namely |glass|ITO|PEDOT:PSS|OC_1C_{10}-PPV:PCBM|LiF/Al|.

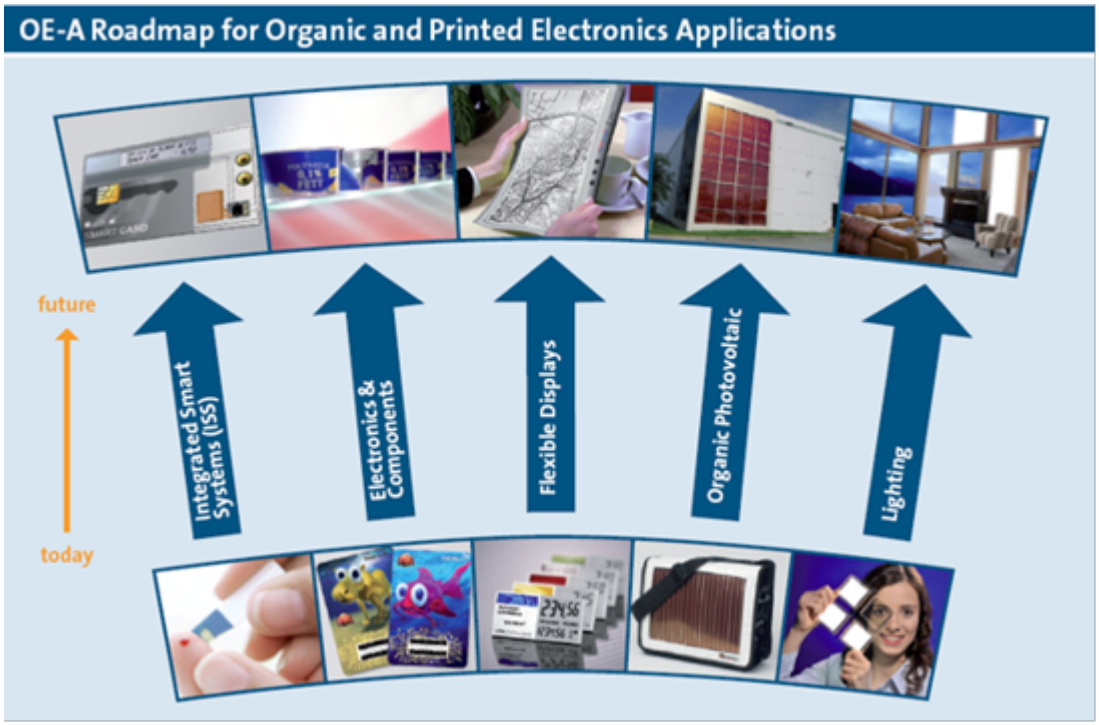

Figure 2.13: Visioned development of organic electronics according to [28, p.1].

> rials and large area, high volume deposition and patterning techniques. Often terms like printed, plastic, polymer, flexible, printable inorganic, large area or thin film electronics - - are used, which essentially all mean the same thing: electronics beyond the classical approach.

In organic photovoltaics, the manufacturing of solar cells using printing processes is one of the most desired features since it would allow fast high yield production which would result in lower manufacturing costs. Printing is allowed if a material can be deposited from solution. These solutions are called *inks*.

Even though organic electronics has several nice features, a few key challenges are limiting this technology's entry in consumer electronics. First thing to be improved is the electrical performance of organic materials. As an example the highest reported conductivity, g, of PEDOT:PSS is $1.418 \cdot 10^5$ S/m [29] which is more than hundred times smaller than the conductivity of copper $g_{\mathrm{Cu}} \approx 6 \cdot 10^7$ S/m (calculated using resistivity of $1.67 \cdot 10^{-8}$ Ωm for copper [4, p.168]). An other big issue that should be overcome in the future is the stability of materials. [28, p.3] Proposed degradation mechanisms include photodegradtion of the active layer and a reaction between the active layer and the electrode material. In addition, preparation and storage of the solar cells in ambient air is known to decrease their performance. [30] The stability issues create a need for proper encapsulation methods — which preferably should be as low-cost as possible.

2.4.1 Electrically conductive polymers

We are used to think of plastics — polymers — as insulating materials, but this view is getting old as conductive polymers are making their way into consumer electronics. The starting point for this technology can be traced back to 1977 when in an article [31] titled *Electrical Conductivity in Doped Polyacetylene*, a "dramatic" increase in the conductivity of polyacetylene via doping was reported. Among authors were Professors Heeger, MacDiarmid and Shirakawa who were awarded with the Nobel Prize in Chemistry in 2000 for their pioneering work in this field. After 1977 Heeger and MacDiarmid continued their work with polyacetylene from which they could build a photoelectrochemical solar cell in 1979 [32]. However it was not until 1990 when a group of scientists from University of Cambridge built a light-emitting diode from poly(*p*-phenylenevinylene) (PPV) that has multiplied and reignited the research activity in the field of conductive polymers. This revolutionary article [33] was authored by Burroughes, Bradley, Brown, Marks, Mackay, Friend, Burns and Holmes and published in Nature titled *Light-emitting diodes based on conjugated polymers*. Above described breakthroughs have allowed the growth of organic electronics into its own field of engineering and form also the basis for our interest — solar cells.

2.4.2 Polymer/fullerene solar cells

Usually it is considered that the benchmark for organic solar cell conversion efficiency was set by Tang in 1985 when he reported in reference [34] a small molecule based heterojunction[5] solar cell with about 1% conversion efficiency. It took long time before polymer solar cells could reach the limit set by Tang. In 1993 Sariciftci et al. reported a heterojunction polymer solar cell using MEH-PPV as donor and C_{60} as acceptor that could reach 0.04 % efficiency. The breakthrough happened in 1995 when Yu et al. presented in reference [22] the first *bulk heterojunction solar cells* that were by two orders of magnitude more efficient than their predecessors, reaching 2.9 percent efficiency [6]. Since then the bulk heterojunction has become standard technology in the field of polymer solar cells. Let us now look more closely at the basic engineering solutions that enable high efficiencies. At the time of writing this thesis Polyera holds the world record in efficiency, 9.1 %, with their polymer/fullerene organic photovoltaic cell. Heliatek has reached 12.0 % with

[5]Often Tang is also incorrectly known as the first one to ever build a heterojunction solar cell. However Tang himself points out in his arcticle that "The first two-layer photovoltaic system appears to be that reported by D.R. Kearns and M. Calvin in J.Chem. Phys. **29**, 950 (1958)"

[6]Yu et al. calculate the efficiency using formula $\eta_e = \frac{FF \cdot V_{oc} I_{sc}}{P_{in}}$, where they define FF as $\int_0^{V_{oc}} IdV$. This results in the following definition for efficiency $\eta_e = \frac{1}{P_{in}} \int_0^{V_{oc}} IdV$ which is different from our definition $\eta = \frac{P_{max}}{P_{in}}$.

their small molecule cell.

Active layer materials

The work horse acceptor material has been the fullerene derivative [6,6]-phenyl-C61-butyric acid methyl ester (PCBM) and a common donor material has been poly(3-hexylthiophene) (P3HT). [18] These materials were chosen to be the active layer materials in this work as well. Originally, fullerene derivatives were preferred over pure C_{60} because of their better solubility and better film forming properties when deposited from solution [22].

Materials that have become more popular just recently include [6,6]-phenyl-C71-butyric-acid methyl ester ($PC_{70}BM$) and poly[*N*-9"-hepta-decanyl-2,7-carbazole-alt-5,5-(4',7'-di-2-thienyl-2',1',3'-benzothiadiazole) (PCDTBT) that were successfully used to produce a solar cell with 6.1 % power conversion efficiency and internal quantum efficiency close to 100 %. The increased efficiency is due to the smaller band gap between donor and acceptor that enables the active layer to absorb a larger fraction of solar spectrum. An other advantage that these materials have over the conventional ones is that they don't require thermal annealing to achieve optimum morphology. [35] (See experimental section 3.2 for more detailed description of preparation of active layers).

Interlayers

Interlayers are used in organic solar cells to better direct the holes and electrons in opposite directions which results in increased current. They fall into two categories: electron injection layers (EIL) and hole injection layers (HIL). An electron selective contact can be achieved by choosing semiconductors whose valence band energies are too low compared to the HOMO level of donor to allow hole injection. A hole selective contact is created by choosing a semiconductor whose conduction band is too high compared to the LUMO level of the acceptor. Obviously, no barrier should exist in order to allow the injection of desired charges. Successfully used EILs have been prepared for example from TiO_x [36] and ZnO [37]. Succesfully used HILs have been made from MoO_3 and V_2O_5 [38]. See section 3 for detailed description of materials used in this work. Figure 2.14 shows the conduction and valence bands of interface layers relative to the donor-acceptor active layer's HOMO and LUMO levels.

The discussion above was about interlayers made of semiconducting materials. Other materials that are known to improve the performance of organic solar cells are, among others, the conductive polymer PEDOT:PSS and caesium carbonate. PEDOT:PSS has been used as an HIL in a same manner than above mentioned

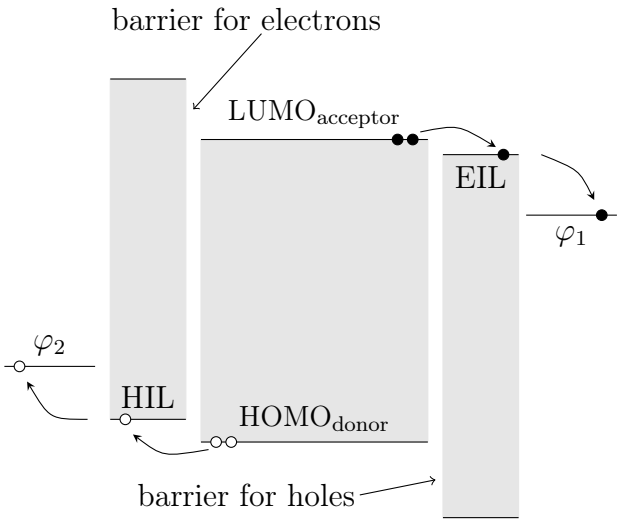

Figure 2.14: Illustration of the energy level alignment of HILs and EILs.

semiconductive materials. Caesium carbonate, however, has the interesting property to be able to alter the work function of the electrode on top of which it is deposited. We will return to these topics in chapter 3.

2.5 Starting point for this work - rectifying junction in Cu organic diodes

The spark for this project was the successful manufacture of printed organic diodes that used copper cathodes. In these devices the semiconductor, PTAA, and the top electrode made of silver ink were gravure printed on a copper cathode which had been sputtered on a PET substrate, giving the diode structure: |Cu|PTAA|Ag|. [39] Since the work functions of silver and copper are both close to the HOMO level of PTAA no rectification should happen under proper bias conditions. It was found that the rectifying behavior was due an initially unintentional dual-dielectric layer between the copper and PTAA. First layer was Cu_2O that was caused by the oxidation of copper and the second dielectric layer resulted from the defects on the PET substrate and perhaps from the PET itself. In the end it was concluded that the method would allow the production of printed organic diodes. [40] Since printing is seen as a way to produce low-cost devices, the scope of this thesis was to study the suitability of copper cathodes for solar cell applications. We also visioned that making the copper bottom electrode work would allow the replacement of expensive ITO cathodes with more affordable copper and thus further reduce the manufacturing costs of solar cells.

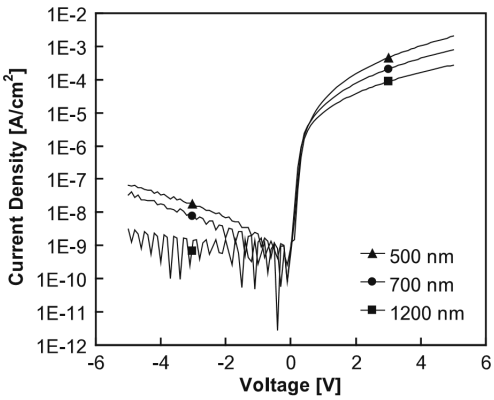

Figure 2.15: IV-curves of Cu|PTAA|Ag-diodes with different semiconductor thicknesses. The copper was sputtered on a PET substrate. Adopted from [39].

3. MATERIALS AND METHODS

In this chapter we introduce all the main materials that were used to build the solar cells studied in this thesis. We also describe the deposition methods. All the studied solar cell structures are presented in figure 3.1.

The solar cells were built on glass substrates, 5 cells on one substrate. The size of the glass substrates was 1 mm × 12 mm × 35 mm. The substrates used in cells *e* and *f* had an ITO coating. Prior to usage all the substrates were cleaned with sonication in acetone, cloroform, sodium lauryl sulfate solution (20 mg sodium lauryl sulfate in 500 ml Milli-Q H_2O), Milli-Q H_2O and 2-propanol for 30 minutes in each solution. Substrates were then dried in vacuum at 150 °C for 1 hour.

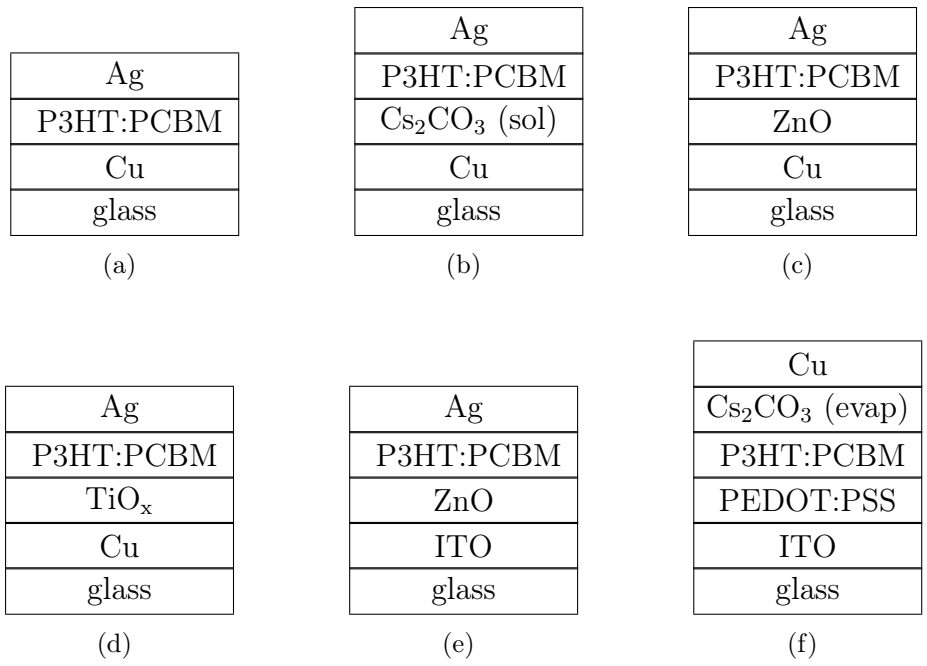

Figure 3.1: Block presentations of every solar cell studied in this thesis. Light enters the cells through the silver electrode in the cells where a copper bottom electrode is used (a–e). In (e–f) light enters the cells through the ITO bottom electrode. Abbreviations sol and evap refer to the deposition methods: solution processing and evaporation.

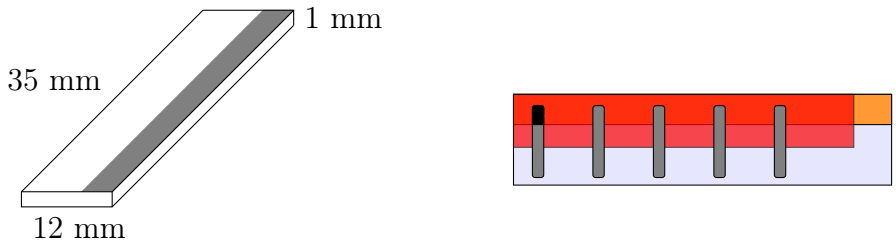

(a) (b)

Figure 3.2: On left is presented the dimensions of a substrate and the shape of a bottom electrode. On right is depicted the way 5 individual solar cells were built on one substrate. Blue color presents the glass substrate, orange the bottom electrode, red the active layer and gray the top electrodes. The active area of the first solar cell is highlighted with black color.

3.1 Electrodes

The shape of the bottom electrode is shown in figure 3.2(a) with gray color. In cells *a-d* (fig.3.1) the copper electrode was evaporated on the cleaned substrates using a mask (Scotch Magic Tape 810) to cover the part that we wanted to keep clean from copper. In cells *e* and *g* the electrode was etched into shape in *aqua regia*

$$\text{Milli-Q } H_2O : HNO_3 : \ HCl = 5 : 0.4 : 4.6$$

in volume ratios. Temperature of the aqua regia bath was 50 °C and bathing time was 7 min. The part of the ITO that we wished to keep was protected with three layers of nail polish.

3.1.1 Copper

Copper in its pure form, Cu, has a work function value in the range of 4.53 eV – 4.94 eV depending on the surface orientation [41, **12**–108]. The work function of the copper cathodes in the diodes discussed in section 2.5 was measured to be 4.8 eV when they were prepared by evaporation [42]. We believe this value is the best estimate for the work function of copper cathodes in our solar cells too.

Copper tends to oxidize easily and it was found out that the Cu electrode of the diodes were covered with a Cu_2O layer [40]. Cu_2O (cuprite or copper(I) oxide) is a semiconducting mineral with a very high resistivity value ranging from 10 Ωm to 50 Ωm [41, **12**–87]. But, due to cuprite's semiconducting property a photoresponse has been obtained in p-Cu_2O/n-ZnO heterostructure films [43]. In that work, the authors got a high control over the crystallographic structure of the Cu_2O layer using rf-magnetron sputtering with a controllable oxygen flow rate and proper post-treatments. They conclude that the well oriented crystallographic structure is the

key factor leading to their success. In the case of the diodes, the cuprite layer grows in an uncontrolled manner on top of the Cu electrode due to the oxygen in our atmosphere.

Copper electrodes were vacuum deposited on cleaned glass substrates. The layers were made 35 nm thick.

3.1.2 Silver

Silver, Ag, has a work function of 4.52 eV to 4.74 eV depending on the surface orientation [41, **12**–108]. The measured value for the silver ink used in the diodes (section 2.5) differs from the value given in the textbooks which is explained to be caused by the oxidation of silver. The measured value for the work function of the silver anode was 5.2 eV. [42] We use this work function value for the silver anodes of our solar cells in this work. The solar cells were illuminated through the silver electrode when the bottom electrode was made of copper. This is possible if the silver layer is not made too thick.

Silver electrodes were vacuum deposited on top of the active layer. The layers were made 25 nm thick.

3.1.3 ITO

ITO, indium tin oxide, films are transparent and electrically conductive which makes them suitable for uses in LED and photovoltaic devices. Actually, ITO has been the choice for electrode material since the dawn of OLED and PLED technology (see for example [44] and [33]), and even before it was used in LCDs.

The work function of around[1] 4.4 eV – 4.5 eV [45] enables the use of ITO as either anode or cathode together with a suitable counter electrode. The *sheet resistance* of the ITO coated glass substrates that we used was 10 Ω/□.

3.1.4 Vacuum deposition

Vacuum deposition is a method to produce thin films with very good control of the thickness of the layers. In the vacuum deposition unit used in this work (Edwards Auto306) the samples, i.e. the solar cells under preparation, are attached to the rotating sample holder that is held from the ceiling of the vacuum chamber.

A suitable amount of a material to be evaporated (Cu, Ag or Cs_2CO_3) is placed in a "cup" made of molybdenum through which an electric current can run. The cups are known as evaporation sources or boats. The current heats up the evaporation boat and the substance, which finally results in the formation of, for example, copper

[1]There is variation in the reported values for ITO work function. For example 4.7 eV is reported in reference [38].

vapor inside the vacuum chamber. The rate at which the material is deposited can be monitored, and was typically few nanometers per minute. Vacuum before the start of the evaporation was typically $\approx 10^{-6}$ mbar.

3.2 Active layer

The active layer was chosen to be donor-acceptor bulk heterojunction type. The donor material used was poly(3-hexylthiophene) i.e. P3HT purchased from Merck under the product name SP001 LISICON and the acceptor material used was [6,6]-phenyl-C61-butyric acid methyl ester i.e. PCBM purchased from Merck under the product name of PV-A600 LISICON.

Preparation

The mass ratio in the final precursor solution that we used for the active layer was

$$\frac{\mathrm{m(PCBM)}}{\mathrm{m(P3HT)}} = \frac{0.8}{1},$$

in which the concentrations, c, of P3HT and PCBM were c(PCBM) = 14.222 mg/ml and c(P3HT) = 17.778 mg/ml.

The final precursor solution was prepared by first measuring PCBM and P3HT in their respective test tubes and dissolving them in 1,2-dichlorobenzene. Argon gas was then injected into the both tubes before closing them. Next the both solutions were stirred for over night at 50 °C with a rate of 500 rmp. Solutions were combined the next morning to give the final precursor described above which was then stirred for 4 h at 70 °C with 300 rpm followed by stirring over night at 50 °C with a rate of 500 rpm. 1 hour before spin coating the temperature of the solution was again increased to 70 °C and the stirring rate to 750 rpm.

Spin coater settings were 500 rpm, 5 min and medium acceleration (012). After spin coating the layers were annealed in vacuum ($\approx 10^{-3}$ mbar) at 110 °C for 10 minutes.

3.2.1 Spin coating

Spin coating is an easy way to produce thin films on small-scale substrates from a precursor solution. The precursor is injected on the substrate which is then spun (10 – 10 000 rmp) to spread the precursor solution on the substrate evenly.

The substrate is held at place with the aid of a vacuum chuck, in other words with suction, on top of which fragment adapters can be employed to have better grip on substrates of different sizes.

The spin coater used in this work was WS-400-6NPP from Laurell Technologies Corporation. Nitrogen flow was set up into the spin coater chamber to protect the samples from impurities and air during the process.

3.3 Interlayers

3.3.1 TiOx

TiO_x can be used as an electron injection layer. It is a semiconductor with conduction band at 4.4 eV and valence band at 8.1 eV. Since for a P3HT:PCBM active layer the HOMO and LUMO bands are at 5.2 eV and 3.7 eV respectively, the titanium oxide can be used as an electron injection layer in a that type of device. [46] It is noteworthy that in reference [46] the enhanced efficiency is attributed to the *optical spacing effect* of the TiO_x layer which is however questioned in [47]. In [36] the improved efficiency is attributed to the proper alignment of band energies of TiO_x — which is the sense we used TiO_x in this work.

Preparation

The instructions for TiO_x synthesis were obtained from private communication with Ph. D. Jin Young Kim and from reference [48]. The method we used is described next.

First an apparatus described in figure 3.3 was set up. All the materials are injected into the flask A from where the final product is collected in the end of the synthesis. The flask B is for collecting the condensed fumes. For the flask A one needs to set up heating, stirring, argon (or nitrogen) gas inlet, material injection and a connection to the condenser. The condenser was water cooled in our set up. For the flask B one needs only a connection to the condenser and an argon (nitrogen) gas outlet. Once the apparatus was set up, an inert environment was created in it by heating the flask A for 2 hours at 120 °C under argon atmosphere and then let cool down to room temperature. Inert atmosphere should be sustained during the whole synthesis.

Materials were injected in order: 5 ml of titanium(IV)isopropoxide, 20 ml of 2-methoxyethanol, 2 ml of ethanolamine. Then, the solution was stirred at room temperature for 1 hour at 250-300 rpm. Next, the temperature was increased to 80 °C and the solution was heated for 1 hour, plus 1 more hour at 120 °C — stirring continuously. Now, the solution was let to cool down. After 30 minutes of heating at 80 °C the solution obtained bluish color and in the end the solution had turned into dark violet color.

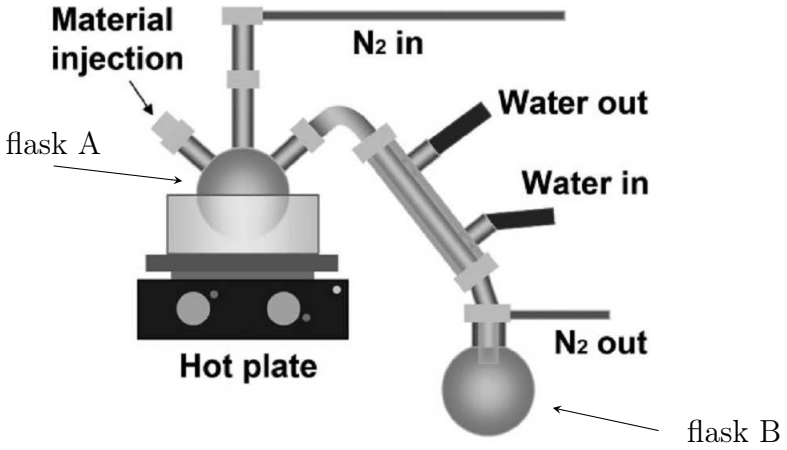

Figure 3.3: The apparatus that was used for TiO_x precursor solution preparation. Adopted from [48].

Next morning[2] the two step heating from 80 °C to 120 °C was repeated and a low-density gel was obtained, as wished for. After the solution had cooled down to room temperature, 10 ml of methanol was injected into the flask A to extract the TiO_x precursor, "the final transparent" (see [48]). The solution separated into two liquid phases of which we collected the upper one.

Solution was spin cast using program: 2000 rpm, 1 min, slow acceleration. The film was then let to hydrolyze in air over night.

3.3.2 PEDOT:PSS

PEDOT:PSS, poly(3,4-ethylenedioxythiophene):poly(styrenesulfonate), is a conductive polymer that can be used as a hole injection layer in P3HT:PCBM devices due its high work function. The conductivity of PEDOT:PSS has been increased up to 1418 S cm^{-1} using ethylene glycol treatment. This high conductivity value allows the use of PEDOT:PSS as a stand alone electrode. [29] The work function of PEDOT:PSS is around 5.2 ± 0.1 eV [49, **19**-27].

3.3.3 ZnO

ZnO can be used an as electron injection layer in a similar manner to TiO_x. The conduction band and valence band energies for ZnO are 4.2 eV and 7.5 eV, respectively [37]. Using the method proposed in [37] the optical transmittance of solution derived ZnO layers can be increased up to 95 %. Solution derived ZnO layers were first introduced to organic photovoltaic device applications in reference [50].

[2]In the instructions the synthesis was completed without pauses

Preparation

Our ZnO precursor solution contained 50 mg/ml of zinc acetate ($C_4H_6O_4Zn \cdot 2H_2O$) dissolved in a solution which was 96 % 2-methoxy ethanol and 4 % ethanolamine. Final product was stirred at 70 °C, 500 rpm for 2 hours and was then let settle down over night. Prior to spin coating the precursor solution was filtered using a 0.2 µm filter. Spin coater settings were 2000 rpm, 1 min and slow acceleration (001).

After spin coating the samples were annealed at 300 °C in air for 5 min and then rinsed with Milli-Q H_2O, ethahol and acetone. As a final step the samples were dried at 300 °C for 3 minutes.

ZnO precursors without the ethanolamine component and without the high temperature annealing were also prepared.

3.3.4 Cesium carbonate

Cesium carbonate (caesium carbonate, *UK*), Cs_2CO_3, can be used to lower the work function of the electrode on which it is deposited. This allows the production of efficient cathodes even from materials that have a considerably high work function. It is also known to enhance the electron injection of usual cathode materials such as aluminum. Interlayers made of Cs_2CO_3 can be prepared by thermal evaporation or by deposition from solution but the properties of the formed layers vary slightly.

It has been shown that *thermally deposited* Cs_2CO_3 decomposes to CsO_2 and cesium suboxides. The formed layer is a n-type semiconductor with high conductivity. The properties of the caesium carbonate films prepared by thermal evaporation are mainly attributed to its decomposition products meaning that the work function of various material's can be modified because a chemical reaction between the electrode material and ceasium carbonate is not needed to lower the work function.

The situation is different when caesium carbonate is deposited using *solution processes* without thermal annealing treatments because then Cs_2CO_3 doesn't decompose into CsO_2. However when caesium carbonate layer is deposited on a reactive metal, such as aluminum, it has been observed to form Al–O–Cs complexes which are able to lower the work function and increase the electron injection properties of the electrode to same extent as thermally evaporated layers of caesium carbonate. Due the desired decomposition products, especially Cs_2O, a thermal annealing treatment has been proposed for solution processed caesium carbonate layers in reference [51]. [52]

Preparation

Cs_2CO_3 layers were deposited either from solution using spin coating or by evaporation. The layer thickness prepared by evaporation was 3 nm. Solution process was

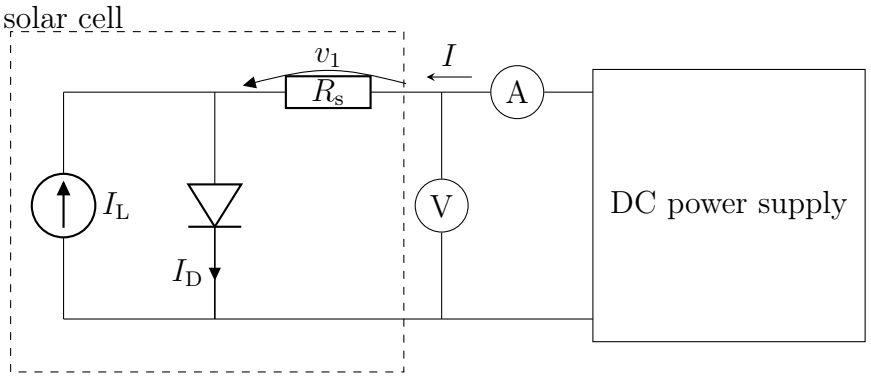

Figure 3.4: SMU measurement of a solar cell under illumination. When the cell is not illuminated $I_L = 0$ and the voltage drop across R_s is reversed. The arrowhead points towards the positive end of the resistor. Equivalent circuit of the solar cell is drawn inside the dashed box.

adopted from reference [51]. The precursor solution was prepared simply dissolving 0.2 weight percent (w%) of Cs_2CO_3 in 2-ethoxyethanol which was then spin coated with settings 2000 rpm, 1 min, slow acceleration. The sample was then heated on a hotplate for 20 minutes at 155 °C.

3.4 Measurement

IV-curves were measured using a Agilent E5272A SMU (Source Measure Unit). SMUs are able to output the sweep voltage or current and measure the dc voltage or current simultaneously.

A simplified set up for a SMU measurement is shown in figure 3.4. The idea is to set a voltage sweep, $V \in [u_{\min}, u_{\max}]$, against the output voltage of the measured sample and then record the value of the output current i at each u to get a set of (u,i)-pairs that graph the IV-curve. The *short circuit current* is obtained when the applied voltage is zero. And the *open circuit voltage* is read from the point where the current is zero. More formally,

$$\begin{aligned} I_{\text{sc}} &= \{i \mid u = 0\} \\ V_{\text{oc}} &= \{u \mid i = 0\}. \end{aligned}$$

Another method get the IV-curve is to connect the output of the solar cell over a variable resistance, $R \in [0, R_{\max}]$ where $R_{\max}$ is so great that practically no current can pass through it and then record all the (u,i)-pairs at each value of R.

Looking at the measured IV-curves given in chapter Results, one sees that they do not quite obey the equation $I = I_0(e^{qV/kT} - 1) - I_L$, and one reason for this is the measurement set up that we are using. When electric current flows through the solar

cell it faces resistance the same way it would do flowing through any material having resistivity different from zero. We call this resistance the series resistance, R_{s}, and we have added it into the equivalent circuit model for the solar cell in figure 3.4. This resistance affects the measurement in different ways during the measurement in dark and under illumination.

The situation under illumination is shown in figure 3.4. When the solar cell is operated in the fourth quadrant, I_{L} is greatest current in the circuit so the net current flows against the direction of I and is thus measured negative. This direction of net current flow causes a voltage drop over the diode and as a result we record a voltage that is smaller than the junction voltage by the amount of the voltage drop, v_1. [53]

Situation is different when the solar cell is measured in dark. Now $I_{\mathrm{L}} = 0$ so the current flows from the DC power supply into the direction of I. Now, since the voltmeter is before the voltage drop v_1, the recorded values for voltage are higher than what actually was applied over the junction. [53] This is one reason why the IV-curves measured under illumination are not simply shifted below the dark curve by the amount of I_{L}, as is predicted by the equation $I = I_0(\mathrm{e}^{qV/kT} - 1) - I_{\mathrm{L}}$.

4. RESULTS AND DISCUSSION

4.1 Copper-active-Ag

A solar cell with structure Cu|P3HT:PCBM|Ag was built to serve as a reference for the experiments with interlayers that will be described in the following sections. 2 out of 10 solar cells worked right after the preparation, but only one after 48 hours. The IV-curve of this solar cell and its performance data is presented in figure 4.1(a) and table 4.1. Figure 4.1(b) shows three representative IV-curves from the same batch that were not able to produce output power.

The open circuit voltage, V_{oc}, of this solar cell is very low, which was expected from theory. Using equation 2.5 we can calculate the predicted open circuit voltage to be

$$V_{\mathrm{oc}} = \frac{\varphi_2 - \varphi_1}{q} = \frac{5.2 \text{ eV} - 4.8 \text{ eV}}{e} = 0.4 \text{ V},$$

which is close to what we got, taking into account the incertitudes in the values used for work functions. If the low voltage was easily explained, the low current density leaves more room for speculation.

The work functions of copper and silver are quite close to each other compared to for example, Al and ITO, Al and PEDOT:PSS, and LiF/Al and ITO which are more common choices for electrode materials and are known to produce high performance devices (see for example [35], [29] and [27]). The small work function difference between copper and silver might not be enough to efficiently transport the electrons and holes to the right electrodes; electrode collected at the anode doesn't contribute positively to the net current. Also, if the electrons and holes are inefficiently lead into opposite directions, that means increased risk of recombination. Finally, the semiconducting, high resistance, Cu_2O layer that grows on top of the copper electrode due oxidation might grow so thick that a major part of current is lost there. Moreover, the oxidation rate is accelerated as a function of temperature. Even though this structure doesn't have interlayers that require annealing treatments, the active layer is heated at 110 °C for 10 minutes in low vacuum ($\approx 10^{-3}$ mbar) during which the copper bottom electrode is also exposed to this temperature. The low oxygen content in the oven of course decelerates the oxidation process. Good treatment on the oxidation of copper is given in [54].

Table 4.1: Performance

Structure	Efficiency %	FF	V_{oc} (V)	J_{sc}(mA/cm^2)
Cu|P3HT:PCBM|Ag	0.30	50	0.30	-0.74

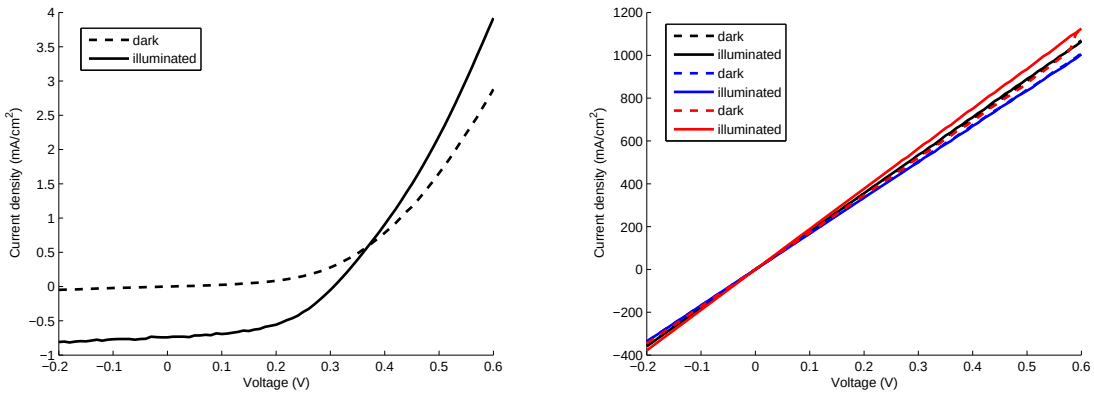

(a) (b)

Figure 4.1: IV-curves of structure Cu|P3HT:PCBM|Ag after 48 hours from preparation. On left, the only one that worked from 10 prepared samples. On right, three representative IV-curves of those that didn't work. Notice that the active layer is still able to inject charges in the solar cell that is marked with red.

From the data plotted in figure 4.1(b) we can calculate the resistance that the current feels going through the actual device of size 0.02 cm^2. The resistance is approximately 30 ohms, which is high enough to exclude the possibility that a direct contact between the electrodes was formed because of careless preparation. But we see that the current is more than 200 times higher compared to the working solar cell which means that low resistance paths from electrode to electrode are formed inside the device at some point during the preparation or before measurement. Looking carefully at the lines marked with red, we see that the current is higher under illumination than in dark which we take as an evidence that the active layer still works and is able to inject charges.

We now propose that the problem is the degradation of the copper electrode — which is initiated by oxidation — and that the active layer is not damaged in any of the structures tested. Next we present an explanation for the lines in figure 4.1(b) and in the following sections we shall be taking a stand on how the interlayer under study did or did not prevent this degrading process from happening.

In reference [55] it was reported that oxygen from the atmosphere penetrates the silver electrode and diffuses trough the device to the back electrode "within a few minutes". This means that the active layer and the silver top electrode are not

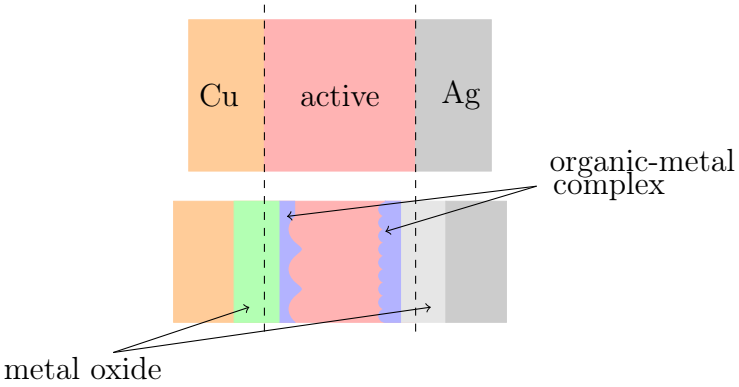

Figure 4.2: We propose that the resistance trough the cell diminishes as a consequence of diffusion of the electrode materials into the active layer. This would explain the high currents in figure 4.1(b).

able to protect the copper from oxidation. Further, it has been shown in [56] that solar cells that use aluminum electrodes thicken by 3.2 nm within 9 hours which is caused by two subsequent processes: 1) formation of aluminum oxide and 2) reaction between aluminum oxide and the organic active layer. The condition for the second reaction to happen is the first one and because we know that a layer of copper oxide is formed in our solar cells, it is then possible that the copper oxide would react with the organic layer. Also, the reaction between silver, which oxidizes too, and the organic layer has not been ruled out. This said, it is now possible that in our Cu|P3HT:PCBM|Ag structure we might have the thickening process going on at both electrodes. As a consequence the reaction products would diffuse into the active layer and this way lower the resistance trough the solar cell. This process is illustrated in figure 4.2. What supports this explanation is the fact that layers in solar cells are known to intermix. Traces of aluminum and indium was found *throughout* a device that was built between aluminum and ITO electrodes. [57].

4.2 Inverted solar cell with solution processed Cs_2CO_3 interlayer

Table 4.2: Performance

Structure	Efficiency %	FF	V_{oc} (V)	J_{sc}(mA/cm^2)
Cu|Cs_2CO_3(sol)|P3HT:PCBM|Ag	0.18	44	0.24	-0.63

In this section we consider a structure Cu|Cs_2CO_3(sol)|P3HT:PCBM|Ag, where the notation Cs_2CO_3(sol) means that the cesium carbonate layer was deposited from solution. The solar cell was built on a glass substrate with evaporated copper

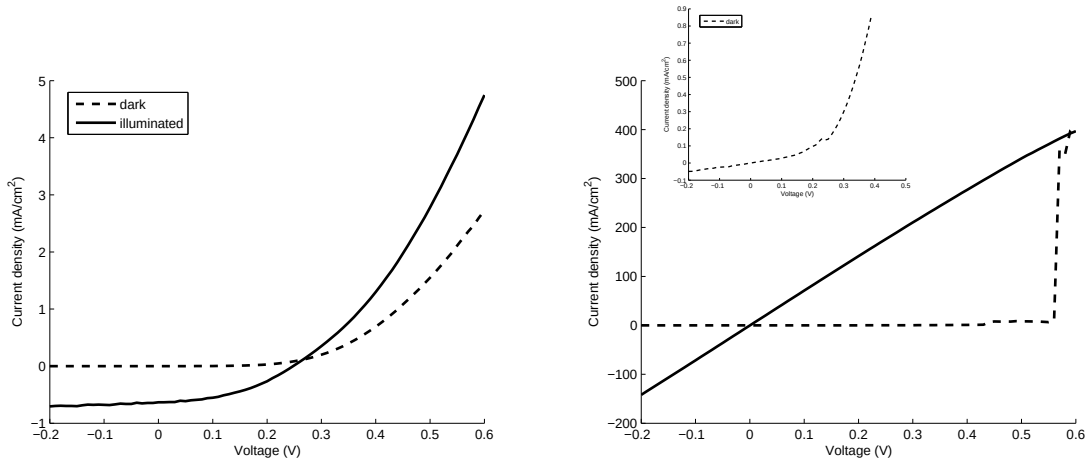

(a) 1 h (b) 15 h

Figure 4.3: IV-curves of a solar cell with structure Cu|Cs_2CO_3 (sol)|P3HT:PCBM|Ag (a) 1 hour and (b) 15 hours after preparation.

bottom electrode. Directly after evaporation of copper, Cs_2CO_3 interlayer and the P3HT:PCBM active layer were deposited from solution, using methods that were described earlier, followed by evaporation of silver top electrode.

Table 4.2 shows the performance of the best cell in the prepared batch and figure 4.3 shows the IV-curves 1 hour and 15 hours after preparation. We see that the performance of the structure is similar to that without the interlayer, but this time 80 % of the cells worked right after preparation. However, degradation of the devices was fast: half of the cells in the batch lost their photovoltaic properties completely in 15 hours as in figure 4.3(b) and the other half showed degraded performance in the measurement.

Figure 4.3(b) reveals us that the problem is in the electrodes, more precisely in the Cu-Cs_2CO_3 electrode since the silver electrode has been proved to work. Silver electrodes are used widely as a part of TUT Department of Chemistry's solar cell research. When measured in the dark, the shape of the IV-curve looks as if it was rectifying which is shown in the inset but actually the leakage current has increased 100 times of what it was right after the preparation, from $1.24 \cdot 10^{-8}$ A to $1.23 \cdot 10^{-6}$ A. However the active layer still clearly works — it is able to inject charges — since the current under illumination has increased from that of dark.

Because we know from measurement that the dark current is not linear, it is clear that the solar cell is not completely short circuited. On the other hand, we see that the current in the cell is higher after 15 hours from preparation than right after which again means that a low resistance path or paths are formed in the cell for the current.

One reason for the poor performance of the device might be that copper is not reactive enough to form Cu–O–Cs complexes; in reference [52] the high efficiency of

devices were attributed to formation of *element*–O–Cs complexes when a solution process was used. In the same work the authors conclude that silver is not reactive enough to form Ag–O–Cs, and were not able to produce efficient PLEDs from Cs_2CO_3 modified silver cathodes. In the periodic table copper is in the same column as silver (and gold) which means that these materials should have *similar chemical properties* [58, p.33], and thus all be not reactive enough for the purpose.

Later in ref [51] it was shown that a thermal annealing treatment would benefit the functioning of solution processed cesium carbonate layers because the Cs_2CO_3 would decompose into CsO_2 which was thought to be the reason for increased performance when thermal evaporation was used. That is why an annealing treatment (20 min, 155 °C in air) was done for all samples. One might think that this extra annealing treatment plus the annealing of the active layer would completely oxidize the copper electrode and prevent the solar cell from working at all, but interestingly 80 % of the prepared solar cells worked as already mentioned which is a considerably higher number of working solar cells than without the cesium carbonate layer.

We explain this improvement in the number of working solar cells with the aid of electrochemistry. (Notice, that in the calculation we are assuming the existence of elemental cesium, Cs, in the film. One might argue if this is actually the case.) Consider the reduction potentials of the following half-reactions [41, p. **8**–17]

$$\begin{array}{rcll} Cu_2O + H_2O + 2\ e^- & \rightarrow & 2\ Cu + 2\ OH^- & E^\circ = -0.360\ V \\ Cs^+ + e^- & \rightarrow & Cs & E^\circ = -3.026\ V \end{array}$$

According to theory, a net reaction that produces a positive voltage difference ΔE° is spontaneous [58, p. 465]. So we get,

$$\begin{array}{rcll} Cu_2O + H_2O + 2\ e^- & \rightarrow & 2\ Cu + 2\ OH^- & E^\circ = -0.360\ V \\ 2\ Cs & \rightarrow & 2\ Cs^+ + 2\ e^- & E^\circ = 3.026\ V \\ \hline Cu_2O + H_2O + 2\ Cs & \rightarrow & 2\ Cu + 2\ OH^- + 2\ Cs^+ & \Delta E^\circ = 2.666\ V \end{array}$$

The positive value after the last reaction means that a reaction where oxidized copper, Cu_2O, is reduced to clean copper, Cu, with the aid of cesium is spontaneous. We believe that this reduction reaction protects the copper electrode during the annealing treatments and some hours after the completion of the solar cell. The solar cells will start degrading because cesium and its compounds are known to be unstable[1] in ambient air [59, p. 308], [60].

For curiosity, solar cells having top electrode from copper were built. The complete structure was ITO|P3HT:PCBM|Cs_2CO_3(evap)|Cu, where (evap) means that

[1] According to [59]: "**Cesium.** – – Oxidizes rapidly in air; in moist air may ignite spontaneously"

Table 4.3: Performance of solar cells where cesium carbonate was evaporated

Structure	Efficiency %	FF	V_{oc} (V)	J_{sc}(mA/cm^2)
ITO|PEDOT:PSS|P3HT:PCBM|Cs_2CO_3 |Cu	1.0	44	0.27	-3.23
ITO|P3HT:PCBM|Cs_2CO_3 |Cu	0.7	43	0.34	-1.83

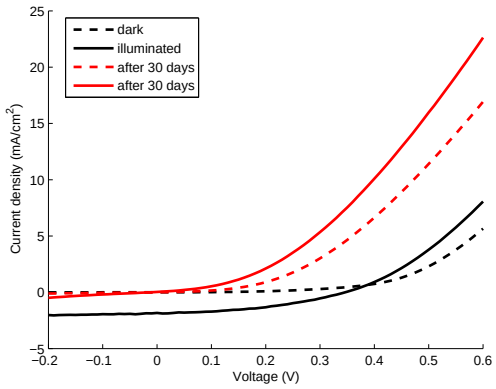

Figure 4.4: IV-curves of ITO|P3HT:PCBM|Cs_2CO_3 (evap)|Cu solar cell right after preparation (dark) and one month after preparation (red).

the cesium carbonate was evaporated. This way the copper electrode wasn't exposed to heating at any point during the process. PEDOT:PSS was used in one batch to enhance the efficiency of the structure. The results are given in table 4.3 and figure 4.4. The obtained efficiencies were higher than in any other structure that we tried because of the transparent ITO electrode through which the cell was illuminated. The interesting observation here is that all the prepared samples were able to keep their rectifying property in dark even one month after the preparation. This observation supports the proposition that annealing treatments accelerate the degrading processes whenever copper electrodes are used.

Another interesting thing is to consider the work functions of ITO and copper that are 4.4 – 4.5 eV and 4.8 eV respectively. Based on these values solely one might expect the ITO to be the cathode. However, the evaporated Cs_2CO_3 is able to lift the work function of copper above ITO's and make the Cu electrode the cathode. This confirms the potential of cesium carbonate as an electrode modifier and broadens the choice of counter electrode materials that could be used with copper. Because the open circuit voltage correlated with the work function difference of the electrodes, this finding now opens the speculations for getting higher voltages from copper cells: using Cs_2CO_3 to lower the work function of copper and choosing a high work function material such as PEDOT:PSS as an anode, might lead to higher voltages and improved efficiency.

Table 4.4: Performance of ITO|ZnO|P3HT:PCBM|Ag

Structure	Efficiency %	FF	V_{oc} (V)	J_{sc}(mA/cm^2)
ITO|ZnO|P3HT:PCBM|Ag	2.44	57	0.54	-2.94

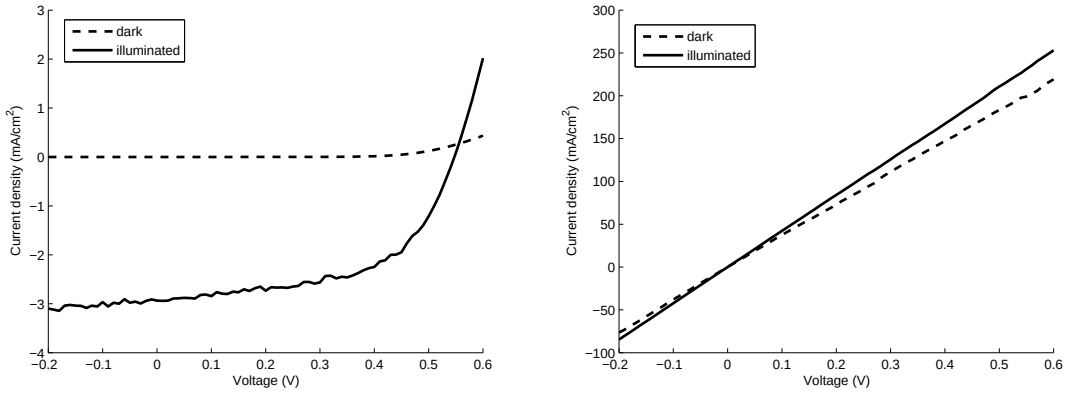

(a) ITO|ZnO|P3HT:PCBM|Ag (b) Cu|ZnO|P3HT:PCBM|Ag

Figure 4.5: a) ZnO precursor without MEA, annealed at 170 °C was shown to work equally efficiently as the standard method. b) This method however didn't work on solar cells having copper electrodes.

4.3 Inverted solar cell with solution processed ZnO interlayer

Attempts to build solar cells with structure Cu|ZnO|P3HT:PCBM|Ag were unsuccessful. The usual method to produce ZnO layers (see section 3.3.3) has been shown to increase the efficiency of organic solar cells in several works. We believe that the method was not suitable for our structure because of the 300 °C annealing temperature and the ethanolamine component used in the precursor solution.

Copper oxidizes in air and the oxidation rate is accelerated as a function of temperature. In our experiments, when the copper electrodes were taken out of the oven their color had turned from copper to green, meaning that they were badly oxidized. The oxidation products, Cu_2O and CuO, are semiconductors with high resistivity. So, when a severe oxidation happens copper loses its property to act as an electrode with a desired work function since it now acts as an insulator.

Ethanolamine (MEA, monoethanolamine) is a strong base [59, p. 3676] and it is said to act as a stabilizer in a ZnO precursor solution [61]. It also allows dissolution of higher zinc acetate concentrations in 2-methoxy ethanol, which was used as a solvent. We observed that precursor solutions which contained the 4 % of ethanolamine damaged the copper electrode immediately when the solution was applied on the electrode surface. It was known that MEA has the ability to dissolve copper and that it has been used in printed circuit board (PCB) etching [62] but

beforehand it was not obvious whether the 4 % in total volume would be crucial amount for our electrodes.

To overcome the problems caused by high temperature annealing and MEA, precursor solutions without MEA were prepared and lower annealing temperatures were tried. It was possible to dissolve 30 mg/ml of zinc acetate in 2-methoxy ethanol without MEA. Using this precursor and 170 °C annealing temperature, solar cells with structure ITO|ZnO|P3HT:PCBM|Ag produced a good photoresponse. A representative IV-curve is given in figure 4.5(a) and the performance data is listed in table 4.4. Even lower annealing temperatures started to decrease the efficiency considerably. The new precursor with 170 °C annealing temperature was tried on Cu|ZnO|P3HT:PCBM|Ag structure, but no rectifying behavior was obtained. We see from the IV-curve (fig. 4.5(b)) that the solar cell reacts to light but is not able to produce any power due to the lack of rectifying property.

In the light of what has been said in the two preceding sections we conclude simply that the ZnO layer is not able to decelerate the degradation processes that will damage the copper electrode. In theory zinc should be able to reduce copper, but it seems that for our purposes the reaction is not strong or fast enough. In the periodic table and in the electrochemical series zinc is closer to copper than cesium or titanium which produced working solar cells, which supports the hypothesis of slow reaction.

4.4 Inverted solar cell with solution processed TiO_x interlayer

In this section we consider a structure Cu|TiO_x|P3HT:PCBM|Ag, where the TiO_x was spin cast from a precursor solution. As a reference, TiO_x was also tested on ITO. The results are summarized in table 4.5 and in figure 4.6. It is seen that, the performance is similar to what we got with structures Cu|P3HT:PCBM|Ag and Cu|Cs_2CO_3 |P3HT:PCBM|Ag ; low voltage is due small work function difference between the electrodes, which also partly explains the small current in addition to the fact that the solar cell is illuminated through 25 nm thick silver electrode. Noteworthy is that the efficiency of the ITO device (3) is relatively low, which might indicate that something went slightly wrong during the synthesis of the precursor meaning that higher efficiencies could be possible achieve.

Again most important findings were obtained in terms of stability. Contrary to any other interlayer we found that TiO_x on top of copper improved the efficiency after one week storage period. Small variations in the J_{sc} value might be caused by variations in the lamp power during the measurement but because the open circuit voltage has increased as well we have a reason to believe that the increase in efficiency can be merited to the TiO_x layer. None of the measured solar cell produced "straight line" IV-curve that we saw with other structures in the previous

sections.

The ability of TiO_x to improve device lifetimes is attributed to its ability to actively remove O_2 and H_2O from a device. Moreover after approximately a one day of storage in air the TiO_x layer transforms from hydrophilic to hydrophobic, and is now able to prevent further intrusion of water or oxygen into the device. The use of TiO_x layer in PLEDs or organic solar cells increases the lifetime of a device approximately two orders of magnitude. [48]

It is thus possible that TiO_x could reduce Cu_2O to Cu owing to its oxygen scavenging property and that it would prevent further flow of oxygen or moisture into the device during storage, which would explain the results we have obtained.

Table 4.5: Performance. The IV-curves of solar cells number 3 and 1 are given in figures 4.6(a) and 4.6(b).

Structure	Efficiency %	FF	V_{oc} (V)	J_{sc}(mA/cm^2)
1 Cu|TiO_x|active|Ag	0.20	45	0.25	-0.67
after a week	0.24	44	0.26	-0.78
2 Cu|TiO_x|active|Ag	0.18	43	0.24	-0.64
after a week	0.19	41	0.27	-0.65
3 ITO|TiO_x|active|Ag	1.32	42	0.38	-3.05
after a week	1.14	41	0.35	-2.93

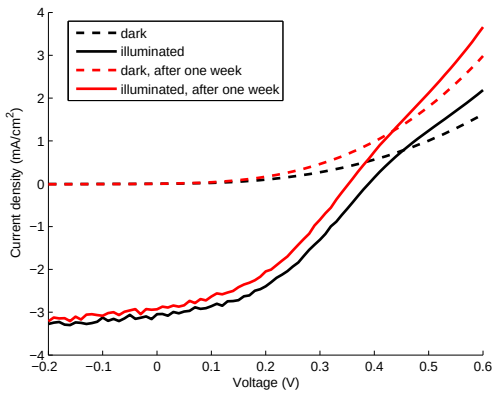

(a) 3 ITO|TiO_x |P3HT:PCBM|Ag

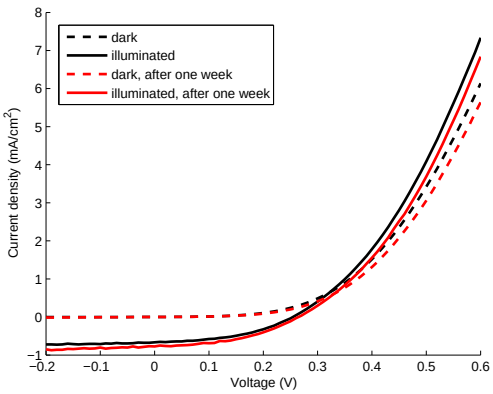

(b) 1 Cu|TiO_x |P3HT:PCBM|Ag

Figure 4.6: Left, ITO/TiO_x reference solar cell suffered from minor degradation during storage time. Right, unlike any other structure that was tested the Cu/TiO_x electrode didn't degrade while stored and was able to produce power even after a one week.

5. CONCLUSIONS

The goal of the present work was to study the suitability of copper as an electrode material in solar cell applications. Four different cases were investigated: a copper electrode without any modification, copper modified by TiO_x, Cs_2CO_3 or ZnO.

It was found out that the thin copper oxide layer that grows in between the electrode and the active layer during the manufacturing process prevents the solar cells from working if the electrode is left unmodified. Deposition of TiO_x or Cs_2CO_3 film on top the copper electrode allows the preparation of working solar cells while ZnO does not.

We proposed that the oxide layer initiates a reaction between the active layer and the electrodes which leads to the diffusion of the electrode materials into the active layer. This process might allow the formation of filament like paths from electrode to electrode that would explain the short circuit like behavior of some of the samples.

In the Cu|PTAA|Ag-diodes that were the inspiration for this work a copper oxide layer is also formed but since the diodes are operated at higher bias voltages, the charges are able to tunnel through the oxide layer. We believe that the few hundred millivolts that we got out of the prepared solar cells is not enough to allow tunneling.

Cesium carbonate and TiO_x allow the production of working solar cells by reducing the oxide layer thickness. But due to the instability of cesium carbonate in air, the solar cells degraded fast. Looking forward, it would be interesting to study whether stability could be achieved by preparing the solar cells under inert atmosphere and using a proper encapsulation. VTT (Technical Research Centre of Finland) has a pilot roll to roll inert atmosphere printing machine [63], so given that stability was achievable via manufacture in inert conditions, the production of printed organic solar cells on copper would be possible.

In the light of this work TiO_x appears to be the most attractive choice as an electrode modifier since it can reduce the oxide layer thickness, it is stable in air and it forms a protective layer which doesn't pass oxygen nor moisture through. In addition, TiO_x doesn't require thermal annealing treatments unlike cesium carbonate or ZnO. We believe that the ZnO layer didn't work because the annealing temperature it requires, is too high for copper.

As a final note we conclude the following: it is possible to prepare organic solar

cells on copper electrodes using a proper electrode modifier for which Cs_2CO_3 and TiO_x were found suitable. For stability, inert manufacture conditions should be studied.

BIBLIOGRAPHY

[1] Climate Change 2007: Synthesis Report. An Assessment of the Intergovernmental Panel on Climate Change. http://www.ipcc.ch/pdf/assessment-report/ar4/syr/ar4_syr.pdf (visited on 12.8.2013)

[2] Decision No 406/2009/EC of The Europian Parliament and of the Council. 23 April 2009. On the effort of Member States to reduce their greenhouse gas emissions to meet the Community's greenhouse gas emission reduction commitments up to 2020. http://eur-lex.europa.eu/LexUriServ/LexUriServ.do?uri=OJ:L:2009:140:0136:0148:EN:PDF (visited on 12.8.2013)

[3] Dave Doody. Basics of Space Flight. National Aeronautics and Space Administration. Available http://www2.jpl.nasa.gov/basics/editorial.php (visited on 12.8.2013)

[4] J.R. Reitz, F.J. Milford and R.W. Christy. Foundations of Electromagnetic Theory. 4th ed. Addison–Wesley, 1993.

[5] G. Dennler, K. Forberich, M. Scharber, C. Brabec, I. Tomis, K. Hingerl, T. Fromherz. Angle dependence of external and internal quantum efficiencies in bulk-heterojunction organic solar cells. J. Appl. Phys. 102 054516 (2007)

[6] M.A. Green. Solar cells: operating principles, technology, and system applications. Kensington: University of New South Wales, 1998.

[7] H.D. Young, R.A. Freedman. Sears and Zemansky's University Physics with Modern Physics. 11th ed. Pearson;Addison-Wesley, 2004.

[8] N. Storey. Electronics a systems approach. 2nd ed. Pearson;Prentice Hall, 1998.

[9] G. L. Pearson and J. Bardeen. Electrical Properties of Pure Silicon and Silicon Alloys Containing Boron and Phosphorus. Physical review, vol. 75 number 5 March 1. 1949.

[10] N.W. Ashcroft, N.D. Mermin. Solid state Physics. Saunders College, 1987.

[11] A.B. Sproul and M.A. Green. Improved value for the silicon intrinsic carrier concentration from 275 to 375 K. J. Appl. Phys. 70, 846 (1991).

[12] B.G. Streetman, S.K. Banerjee. Solid state electronic devices. 6th ed. Pearson;Prentice Hall, 2006.

[13] D.M. Chapin, C.S. Fuller, and G L. Pearson. A New Silicon pn Junction Photocell for Converting Solar Radiation into Electrical Power. J. Appl. Phys. 25, 676 (1954).

[14] M.B. Prince. Silicon Solar Energy Convertes. J. Appl. Phys. 26 534-540 (1955).

[15] Tian Hanmina, Zhang Xiaoboa, Yuan Shikuia, Wang Xiangyana, Tian Zhipenga, Liu Bina, Wang Yinga, Yu Taoa, Zou Zhiganga. An improved method to estimate the equivalent circuit parameters in DSSCs. Solar Energy 83 715–720 (2009).

[16] A. Cheknane, H. S. Hilal, F. Djeffal, B. Benyoucef, J-P Charles. An equivalent circuit approach to organic solar cell modeling. Microelectronics Journal 39 1173-1180 (2008).

[17] B. A. Gregg and M. C. Hanna. Comparing organic to inorganic photovoltaic cells: Theory, experiment, and simulation. J. Appl. Phys. 93, 3605 (2003).

[18] G. Dennler and N. Sariciftci. Flexible Conjugated Polymer-Based Plastic Solar Cells: From Basics to Applications. Proceedings of the IEEE (Volume:93 , Issue: 8) 1429 - 1439 (2005).

[19] Blom, Mihailetchi, Koster and Markov (2007), Device Physics of Polymer:Fullerene Bulk Heterojunction Solar Cells. Adv. Mater., 19: 1551-1566.

[20] J. Kniepert, M. Schubert, J. C. Blakesley, D. Neher. Photogeneration and Recombination in P3HT/PCBM Solar Cells Probed by Time-Delayed Collection Field Experiments. Journal of Physical Chemistry Letters J. Phys. Chem. Lett., 2 (7), pp 700–705 (2011).

[21] Steve Albrecht, Wolfram Schindler, Jona Kurpiers, Juliane Kniepert, James C. Blakesley, Ines Dumsch , Sybille Allard , Konstantinos Fostiropoulos , Ullrich Scherf , and Dieter Neher. On the Field Dependence of Free Charge Carrier Generation and Recombination in Blends of PCPDTBT/$PC_{70}BM$: Influence of Solvent Additives. J. Phys. Chem. Lett. , 2012, 3 (5), pp 640–645

[22] G. Yu, J. Gao, J. C. Hummelen, F.Wudl, A.J. Heeger. Polymer Photovoltaic Cells: Enhanced Efficiencies via a Network of Internal Donor-Acceptor Heterojunctions. Science, New Series, Vol.270, No. 5243 (Dec. 15, 1995), 1789-1791.

[23] A. Haugeneder, M. Neges, C. Kallinger, W. Spirkl, U. Lemmer, and J. Feldmann, U. Scherf, E. Harth, A. Gügel, and K. Müllen. Exciton diffusion and dissociation in conjugated polymer/fullerene blends and heterostructures. Phys. Rev. B 59, 15346–15351 (1999).

[24] L. J. A. Koster, E. C. P. Smits, V. D. Mihailetchi, and P. W. M. Blom . Device model for the operation of polymer/fullerene bulk heterojunction solar cells. Phys. Rev. B 72, 085205 (2005).

[25] W. Shockley and H. J. Queisser. Efficiency of a p-n Junction Solar Cells. J. Appl. Phys. 32, 510-519 1961.

[26] V. D. Mihailetchi, P. W. M. Blom, J. C. Hummelen, and M. T. Rispens. Cathode dependence of the open-circuit voltage of polymer:fullerene bulk heterojunction solar cells. J. Appl. Phys. 94, 6849 (2003).

[27] Scharber, Mühlbacher, Koppe, Denk, Waldauf, Heeger and Brabec,(2006), Design Rules for Donors in Bulk-Heterojunction Solar Cells — Towards 10% Energy-conversion Efficiency. Adv. Mater., 18: 789-794.

[28] White Paper "Roadmap for Organic and Printed Electronics". 4th ed. 2011. Available at `http://www.oe-a.org/en_GB/downloads`. (visited on 16.8.2013)

[29] Kim, Y. H., Sachse, C., Machala, M. L., May, C., Müller-Meskamp, L. and Leo, K. (2011), Highly Conductive PEDOT:PSS Electrode with Optimized Solvent and Thermal Post-Treatment for ITO-Free Organic Solar Cells. Adv. Funct. Mater., 21: 1076–1081

[30] Pathways for the degratation of organic photovoltaic P3HT:PCBM based devices. Matthew O. Reese, Anthony J. Morfa, Matthew S. White, Nikos Kopidakis, Sean E. Shaheen, Garry Rumbles, David S. Ginley. Solar Energy Materials 6 Solar Cells 92 (2008) 746–752.

[31] C. Chiang, C. Fincher, Y. Park, A. Heeger, H. Shirakawa, E. Louis, S. Gau, A. MacDiarmid. Electrical conductivity in doped polyacetylene. Physical review letters. vol. 39. number 17. 1977.

[32] S.N. Chen, A.J. Heeger, Z. Kiss, A. G. MacDiarmic, S. C. Gau and D.L. Peebles. Polyacetylene, $(CH)_x$:Photoelectrochemical solar cell. Appl. Phys. Lett. 36, 96 (1980)

[33] Light-emitting diodes based on conjugated polymers. J.H. Burroughes, D. D. C. Bradley, A. R. Brown, R. N. Marks, K. Mackay, R. H. Friend, P. L. Burns & A. B. Holmes. Nature 347, 539 - 541 11 October (1990).

[34] C.W. Tang. Two-layer organic photovoltaic cell. Appl. Phys. Lett. 48, 183 (1986).

[35] Sung Heum Park, Anshuman Roy, Serge Beaupré, Shinuk Cho, Nelson Coates, Ji Sun Moon, Daniel Moses, Mario Leclerc, Kwanghee Lee & Alan J. Heeger. Bulk heterojunction solar cells with internal quantum efficiency approaching 100 % Nature Photonics 3, 297 - 302 (2009).

[36] C. Waldauf, M. Morana, P. Denk, P. Schilinsky, K. Coakley, S. A. Choulis, and C. J. Brabec. Highly efficient inverted organic photovoltaics using solution based titanium oxide as electron selective contact. Appl. Phys. Lett. 89, 233517 (2006).

[37] A. K. K. Kyaw, X. W. Sun, C. Y. Jiang, G. Q. Lo, D. W. Zhao, and D. L. Kwong. An inverted organic solar cell employing a sol-gel derived ZnO electron selective layer and thermal evaporated MoO_3 hole selective layer. Appl. Phys. Lett. 93, 221107 (2008).

[38] Vishal Shrotriya, Gang Li, Yan Yao, Chih-Wei Chu, and Yang Yang. Transition metal oxides as the buffer layer for polymer photovoltaic cells. Appl. Phys. Lett. 88, 073508 (2006).

[39] Kaisa E. Lilja, Tomas G. Bäcklund, Donald Lupo, Tomi Hassinen, Timo Joutsenoja. Gravure printed organic rectifying diodes operating at high frequencies, Organic Electronics Volume 10, Issue 5, August 2009, Pages 1011–1014.

[40] K E Lilja, H S Majumdar, K Lahtonen, P Heljo, S Tuukkanen, T Joutsenoja, M Valden, R Österbacka and D Lupo. Effect of dielectric barrier on rectification, injection and transport properties of printed organic diodes. J. Phys. D: Appl. Phys. 44 295301

[41] David R. Lide. CRC Handbook of Chemistry and Physics 73^{rd} ed. CRC Press, 1992.

[42] Kaisa E. Lilja, Himadri S. Majumdar, Fredrik S. Pettersson, Ronald Österbacka, and Timo Joutsenoja. Enhanced Performance of Printed Organic Diodes Using a Thin Interfacial Barrier Layer. ACS Appl. Mater. Interfaces, 2011, 3 (1), pp 7–10

[43] K. Akimoto, S. Ishizuka, M. Yanagita, Y. Nawa, Goutam K. Paul, T. Sakurai. Thin film deposition of Cu_2O and application for solar cells. Solar Energy 80 (2006) 715-722.

[44] C.W. Tang and S. A. VanSlyke. Organic electroluminescent diodes. Appl. Phys. Lettr. 51 (12), 1987.

[45] Y. Park, V. Choong, Y. Gao, B. R. Hsieh, C.W. Tang. Work function of indium tin oxide transparent conductor measured by photoelectron spectroscopy. Appl. Phys. Lett. 68, 2699 (1996).

[46] J. Y. , S. H. Kim, H.-H. Lee, K. Lee, W. Ma, X. Gong, A. J. Heeger. New Architecture for High-Efficiency Polymer Photovoltaic Cells Using Solution-Based Titanium Oxide as an Optical Spacer. Volume 18, Issue 5, pages 572–576, March, 2006.

[47] Tayebeh Ameri, Gilles Dennler, Christoph Waldauf, Patrick Denk, Karen Forberich, Markus C. Scharber, Christoph J. Brabec, and Kurt Hingerl. Realization, characterization, and optical modeling of inverted bulk-heterojunction organic solar cells. J. Appl. Phys. 103, 084506 (2008).

[48] Shinuk Cho, Kwanghee Lee, Alan J. Heeger. Extended Lifetime of Organic Field-Effect Transistors Encapsulated with Titanium Sub-Oxide as an 'Active' Passivation/Barrier Layer. Adv. Mater. 2009, 21, 1941-1944.

[49] Conjugated Polymers: Theory, Synthesis, Properties, and Characterization (Handbook of Conducting Polymers, Third Edition)

[50] M. S. White, D. C. Olson, S. E., Shaheen, N. Kopidakis, and D. S. Ginley. Inverted bulk-heterojunction organic photovoltaic device using a solution-derived ZnO underlayer. Appl. Phys. Lett. 89, 143517 (2006).

[51] Hua-Hsien Liao, Li-Min Chen, Zheng Xu, Gang Li, and Yang Yang. Highly efficient inverted polymer solar cell by low temperature annealing of Cs_2CO_3 interlayer. Appl. Phys. Lett. 92, 173303 (2008)

[52] Jinsong Huang, Zhen Xu, and Yang Yang. Low-Work-Function Surface Formed by Solution-Processed and Thermally Deposited Nanoscale Layers of Cesium Carbonate. Adv. Funct. Mater. 2007, 17, 1966-1973

[53] M. Wolf and H. Rauschenbach. Series Resistance Effects on Solar Cell Measurement. (Advanced Energy Conversion, April–June 1963)

[54] T.N. Rhodin Jr. Low Temperature Oxidation of Copper. I. Physical Mechanism. Journal of the American Chemical Society 1950 72 (11), 5102-5106.

[55] Monica Lira-Cantu, Kion Norrman, Jens W. Andreasen, and Frederik C. Krebs. Oxygen Release and Exchange in Niobium Oxide MEHPPV Hybrid Solar Cells. Chem. Mater. 2006, 18, 5684–5690.

[56] B. Paci, A. Generosi, V. Rossi Albertini, P. Perfetti, R. Bettignies, J. Leroy, M. Firon, C. Sentein. Controlling photoinduced degradation in plastic photovoltaic cells: A time-resolved energy dispersive x-ray reflectometry study. Appl. phys. lettr. 89, 043507 (2006)

[57] Frederik C. Krebs and Kion Norrman. Analysis of the Failure Mechanism for a Stable Organic Photovoltaic During 10 000 h of Testing. Progress in photovoltaics: research and applications 2007;15:697–712.

[58] S.S. Zumdahl. Chemical principles. 4th ed. Houghton Mifflin Company, 2002.

[59] The Merck Index, An Encyclopedia of Chemicals, Drugs, and Biologicals. 11th ed. Merck & Co., Inc., 1989

[60] T. R. Briere and A. H. Sommer. Low-work-function surfaces produced by cesium carbonate decomposition. Journal of Applied Physics 48, 3547 (1977).

[61] Jin-Hong Lee, Kyung-Hee Ko, Byung-Ok Park. Electrical and optical properties of ZnO transparent conducting films by the sol–gel method. Journal of Crystal Growth Volume 247, Issues 1–2, January 2003, Pages 119–125.

[62] C-W. SHIH, Y-Y. Wang and C-C. WAN. Study of the mechanism of additives on copper dissolution in monoethanolamine-complexed cupric ion solution. Journal of Applied Electrochemistry 32: 987-992, 2002.

[63] VTT (Technical Research Centre of Finland) Home Page `http://www.vtt.fi/service/roll_to_roll_processing.jsp?lang=en` (visited on 12.8.2013)